Horizon 2020 Societal challenge 5:
Climate action, environment, resource efficiency and raw materials

VERIFY

Observation-based system for monitoring and verification of greenhouse gases

GA number 776810, RIA

Deliverable number (relative in WP)	**D2.8**
Deliverable name:	Source sector dominated proxy/ffCO_2 ratios
WP / WP number:	2
Delivery due date:	Month 36 (31/01/2021)
Actual date of submission:	Month 48 (21/01/2022)
Dissemination level:	Public
Lead beneficiary:	UHEI
Responsible	S. Hammer (UHEI)
Contributor(s):	C. Rosendahl (UHEI), C. Alberti (KIT), F. Hase (KIT), S. Hammer (UHEI)
Internal reviewer:	P.Peylin (LSCE), G.Moulas (ARTTIC)

Changes with respect to the DoA
Due to the Coronavirus pandemic, the field campaigns have been delayed. The final deliverable was submitted in January 2022.
Dissemination and uptake (Who will/could use this deliverable, within the project or outside the project?)
The proxy/ffCO$_2$ results derived in this report will be used as: • Independent validation information for inventory-based proxy/ffCO$_2$ emission ratios (TNO: Task 2.1) • Input to derive proxy-based continuous ffCO$_2$ estimates in the Rhine Valley test area for the inverse modelling in Task 2.4.3. • Assess the variability of the proxy/ffCO$_2$ ratios and thus the uncertainty of proxy-based ffCO$_2$ estimates (T2.4.3)
Short Summary of results (<250 words)
We investigate source sector dominated proxy/ffCO$_2$ ratios with in-situ and total column measurements. The studied proxies are CO, NO$_2$ and NO$_x$. Three independent campaigns were performed: one in-situ campaign targeting the residential heating sector as well as two, one in-situ and one remote sensing campaign for the traffic sector. For the heating sector, we found a mean $\Delta CO/\Delta ffCO_{2\ (heating)}$ ratio of 6.5 ± 2.6 ppb/ppm and a concurrent mean $\Delta NO_x/\Delta ffCO_{2\ (heating)}$ ratio of 0.8 ± 0.2 ppb/ppm. Both ratios are 2 to 4 times higher compared to inventory-based residential heating emission ratios in the municipality. The mismatch decreases to a 50% underestimation of the inventory when compared to the averaged proxy/ffCO$_2$ emission ratios predicted by the TNO inventory in a 50 km x 50 km surrounding of Heidelberg. Especially the $\Delta CO/\Delta ffCO_{2\ (heating)}$ ratio showed a large variability of 40% (1σ). The observed variabilities in the atmospheric ratios are underestimated by the inventory for the CO/ffCO$_2$ emission ratio but overestimated for NO$_x$/ffCO$_2$. For the traffic sector, the remote sensing campaign was unable to detect Δproxy/ΔXCO$_2$ ratios. The signals from highway traffic emissions were too weak to be detected by total column observations with their current precision. The in-situ campaign performed close to the highway revealed a mean $\Delta CO/\Delta ffCO_{2\ (traffic)}$ ratio of 5.21 ± 1.01 ppb/ppm along with a mean $\Delta NO_x/\Delta ffCO_{2\ (traffic)}$ ratio of 2.24 ± 0.25 ppb/ppm. The experimentally determined ratios are, within their uncertainties, consistent with inventory-based traffic emission ratios if a different gasoline and diesel emissions distribution is assumed.
Evidence of accomplishment (report, manuscript, web-link, other)
Report

VERIFY is a research project funded by the European Commission under the H2020 program. Grant Agreement number 776810.

Version	Date	Description	Author (Organisation)
V0	20/01/2021	Creation/Writing	C. Rosendahl (UHEI) Carlos Alberti (KIT) Frank Hase (KIT) S. Hammer (UHEI)
V0.1	29/01/2021	Writing/Formatting/Delivery	C. Rosendahl (UHEI) S. Hammer (UHEI)
V0.2	30/06/2021	Writing/Formatting/Delivery	C. Rosendahl (UHEI) S. Hammer (UHEI)
V1	21/01/2022	Formatting/Delivery on the Participant Portal	F. Chevalier (LSCE/CEA) G.Moulas (ARTTIC)

VERIFY is a research project funded by the European Commission under the H2020 program. Grant Agreement number 776810.

VERIFY is a research project funded by the European Commission under the H2020 program. Grant Agreement number 776810.

1. Glossary

Abbreviation / Acronym	Description/meaning
$^{14}CO_2$	carbon dioxide containing the isotope ^{14}C
A5	investigated highway A5 with North-South orientation
asl	above sea level
COVID	COrona VIrus Disease
COCCON	Collaborative Carbon Column Observing Network
$\delta^{13}C$	relative difference between isotopic $^{13}C/^{12}C$ ratio of sample and standard according to Mook [Mook, 1986]
$\Delta^{14}C$	$^{14}C/C$ ratio expressed in Δ notation according to Stuvier and Polach [Stuvier and Polach, 1977]
ΔCO_2, ΔCO, ΔNO_x	concentration enhancement with respect to a background
DOAS	Differential Optical Absorption Spectroscopy
EM27/SUN	Fourier Transform Infrared Remote Sensing spektrometer
ffCO_2	Fossil fuel CO_2
FTIR	Fourier Transform Infrared
GHGs	Greenhouse gases
ICAD	Iterative CAvity enhanced DOAS instrument for NO_x and NO_2
ICOS FCL	Integrated Carbon Observation System Flask and Calibration Laboratory
KIT	Karlsruhe Institute for Technology
LUBW	regional office for environmental issues, federal state of Baden-Württemberg; mentioned in reference to its emission inventory
ML1/ML2	Mobile Laboratory one and two
NO_x	sum of NO and NO_2
StaLA	State Statistical Office of federal state of Baden-Württemberg; mentioned in reference to its emission inventory
TCCON	Total Carbon Column Observing Network
TNO	Netherlands Organisation for Applied Scientific Research, mentioned in reference to its emission inventory
UHEI	University of Heidelberg
UTC	Coordinated Universal Time
VOC	Volatile Organic Compound
XCO_2, XCO	Dry air molar gas fractions, e.g. XCO_2, XCO

VERIFY is a research project funded by the European Commission under the H2020 program. Grant Agreement number 776810.

2. Executive Summary

Observation-based fossil fuel CO_2 ($ffCO_2$) estimates provide important information to atmospheric inverse modelling frameworks to evaluate the modelled contributions of fossil and non-fossil CO_2 sources and sinks. Finding the "correct" share of fossil and non-fossil CO_2 sources is essential for the interpretation of biogenic carbon sources and sinks, as well as the estimate of $ffCO_2$ emissions. Radiocarbon (^{14}C) observations of atmospheric CO_2 are the most direct measurements to estimate the $ffCO_2$ share. However, $^{14}CO_2$-based $ffCO_2$ estimates are sparse, both temporally and spatially, as still today $^{14}CO_2$ can only be analysed based on flask samples since no continuous $^{14}CO_2$ instrument with the necessary precision is available yet.

Apart from $^{14}CO_2$, co-emitted species are used for proxy-based $ffCO_2$ estimates. While proxy-based estimates do not reach the precision of the ^{14}C-based estimates, proxies can be measured continuously and even with remote sensing techniques, extending this approach to estimate $ffCO_2$ potentially towards space-based observations. Proxy-based $ffCO_2$ estimates rely on knowing the different proxy/$ffCO_2$ emission ratios for different $ffCO_2$ combustion processes and the ability to account for the proxies' atmospheric chemistry correctly. State-of-the-art emission inventories account for different proxy/$ffCO_2$ ratios for different $ffCO_2$ source sectors and even variations within those sectors. This report aims to observe Δproxy/$\Delta ffCO_2$ ratios in the atmosphere for specific emission sectors and compare them to the emission inventories' proxy/$ffCO_2$ emission ratios.

We investigate the proxy/$ffCO_2$ emission ratios from the residential heating and traffic sector using CO and NO_x as proxies. We conduct dedicated measurement campaigns to observe the effective atmospheric Δproxy/$\Delta ffCO_2$ ratios, thus intrinsically considering atmospheric chemistry for the in-situ and the ground-based total column measurements. The campaigns were designed to temporally and spatially separate the source sector of interest from influence by non-targeted source sectors.

The first in-situ campaign was dedicated to the atmospheric Δproxy/$\Delta ffCO_2$ ratios of the residential heating sector and found the following mean ratios:

$$\Delta CO/\Delta ffCO_{2\ (heating)} = 6.5 \pm 2.6 \text{ ppb/ppm}$$
$$\Delta NO_x/\Delta ffCO_{2\ (heating)} = 0.80 \pm 0.15 \text{ ppb/ppm}$$

Both ratios are 2 to 4 times higher compared to inventory-based residential heating emission ratios in the municipality. The mismatch decreases to a 50% underestimation of the inventory when compared to the averaged proxy/$ffCO_2$ emission ratios predicted by the TNO inventory in a 50 km x 50 km surrounding of Heidelberg. Especially for the mean $\Delta CO/\Delta ffCO_{2\ (heating)}$ ratio, we observe a large variability of 40% (1σ) that is, however, expected as the different heating fuel-types (oil, gas and wood) have very different CO/$ffCO_2$ ratios. The variability in $NO_x/ffCO_2$ ratio is, at the same time, less than 20% (1σ). The variabilities of the atmospheric Δproxy/$\Delta ffCO_2$ ratios

VERIFY is a research project funded by the European Commission under the H2020 program. Grant Agreement number 776810.

differ significantly from the variabilities assumed in the inventory. The TNO inventory underestimates the CO/ffCO$_2$ variability and overestimates the NO$_x$/ffCO$_2$ variability.

We conducted two highway traffic campaigns, one in-situ and one remote sensing. Highway traffic emissions were too weak to be detected by total column observations with their current precision. In-situ campaigns performed close to the highway revealed the following mean Δproxy/ΔffCO$_2$ ratios:

$$\Delta CO/\Delta ffCO_{2\,(traffic)} = 5.21 \pm 1.01 \text{ ppb/ppm}$$
$$\Delta NO_x/\Delta ffCO_{2\,(traffic)} = 2.24 \pm 0.25 \text{ ppb/ppm}$$

The reported mean ΔCO/ΔffCO$_{2\,(traffic)}$ and ΔNO$_x$/ΔffCO$_{2\,(traffic)}$ ratios are within their uncertainties, consistent with inventory-based traffic emission ratios for highway driving conditions if a different gasoline and diesel emissions mix, with a larger gasoline share, is assumed.

Apart from serving as independent validation for the emission inventories, the observations provide a measure for the variability of the source dominated Δproxy/ΔffCO$_2$ ratios which feed directly into the uncertainty of the proxy-based ffCO$_2$ estimates. Furthermore, the proxy/ffCO$_2$ emission ratios determined here have a local validity and will thus be used to calculate the proxy-based continuous ffCO$_2$ estimates and their uncertainties needed for the inverse modelling of the ffCO$_2$ sources in the Rhine valley test area in Task 2.4.3.

VERIFY is a research project funded by the European Commission under the H2020 program. Grant Agreement number 776810.

3. Introduction

Atmospheric trace gas species, which are co-emitted along with fossil fuel CO_2 ($ffCO_2$) emissions, have been studied for decades and help to improve the ability to detect $ffCO_2$ concentration enhancements ($\Delta ffCO_2$) in the atmosphere. These co-emitted species, also called $ffCO_2$ proxies, are used for different purposes. In the following, we list three examples of how proxies have been used to expand and improve the interpretation of $ffCO_2$ observations:

- Improve the temporal resolution of $\Delta ffCO_2$ [Levin and Karstens, 2007]
- Sectoral attribution of $\Delta ffCO_2$ [Turnbull et al., 2015]
- Spatial localisation of $\Delta ffCO_2$ plumes, estimation of $\Delta ffCO_2$ emissions from satellite measurements [Reuter et al., 2019, Konovalov et al., 2016]

$^{14}CO_2$-based $ffCO_2$ estimates are the most direct atmospheric fossil fuel detection method; however, they are costly and laborious. Consequently, $^{14}CO_2$-based $ffCO_2$ measurements are temporally (and spatially) sparse. Levin and Karstens, (2007) showed that continuous CO measurements can be used as a proxy for regional $\Delta ffCO_2$. They estimated uncertainties between 20% and 40% for hourly $ffCO_2$ values. Each major emission sector (power plants & industry, residential heating, and traffic) has specific proxy/$\Delta ffCO_2$ ratios. Turnbull et al. (2015) used characteristic CO/$\Delta ffCO_2$ ratios to identify the contribution of different source sectors over the course of a day. The measurements have also been used to evaluate the inventory-based CO/$ffCO_2$ ratios for the traffic sector. In satellite studies, proxy measurements are used for constraining the spatial extent of urban or industrial CO_2 plumes [Reuter et al., 2019]. Konovalov et al. (2016) developed an inverse modelling method using satellite proxy measurements and emission inventory NO_x/$ffCO_2$ ratios to estimate $ffCO_2$.

These examples demonstrate the broad application range of $ffCO_2$ proxies. All applications build on the co-emission of $ffCO_2$ and the proxies during the combustion of fossil fuels. CO and NO_x are the most commonly used $ffCO_2$ proxies. CO is produced during incomplete combustion of fossil - but also biofuels. NO_x has different formation pathways (1) by a thermal reaction between N_2 and O_2 (thermal NO), (2) by CH_n radicals (prompt NO), or (3) from fuel nitrogen [Glarborg et al. 2018]. According to Smooke et al. [Smooke et al., 1996], prompt NO is the dominant source of NO in hydrocarbon/air diffusion combustion. The emission of both proxies CO and NO_x depend thus on combustion temperature, efficiency and fuel type. Therefore, different fossil fuel emission sectors have different proxy/$ffCO_2$ ratios.

While for the period of interest (a few hours to days), CO can be regarded as a chemically stable proxy, this is not the case for NO_x. NO_x has a complex and variable chemical lifetime depending on, e.g., the NO_x concentration itself, OH, VOC and ozone concentrations, as well as sunlight availability [Seinfeld & Pandis 2016]. During winter, the NO_x lifetime varies between 6.3 h during night and 29 h during daytime [Kenagy et al., 2018]. For summer, Shah et al. (2020) give an average lifetime is 5.9 h, not differentiating between day and night.

VERIFY is a research project funded by the European Commission under the H2020 program. Grant Agreement number 776810.

In order to take into account the complex air chemistry of NO_x, we aim to determine effective atmospheric Δproxy/ΔffCO$_2$ ratios for both in-situ and total column observation. We strive to determine Δproxy/ΔffCO$_2$ ratios dominated by one emission sector through a careful and rigorous selection of the measurement locations and times. Understanding the effective atmospheric ratios and their variability for different source sectors is an essential prerequisite for a potential, future quantitative use of CO and NO_x as proxies for ffCO$_2$ once the air chemistry modelling capabilities have reached the required level of refinement.

Practically, we measure the atmospheric Δproxy/ΔffCO$_2$ ratios using two mobile in-situ laboratories (UHEI) and two total column spectrometers (KIT). The in-situ measurements investigate ΔCO/ΔffCO$_2$ and $\Delta NO_x/\Delta$ffCO$_2$ ratios while the total column measurement investigates ΔXCO/ΔXCO$_2$ ratios. Three independent campaigns were conducted: one focusing on residential heating emissions (UHEI, in-situ), and two focusing on the traffic sector, using both total column (KIT) and in-situ observations (UHEI).

This report summarises previous source-specific proxy/ffCO$_2$ studies from the literature and briefly discusses their level of consistency. We then present the applied experimental approaches as well as the instrumentation used. Finally, the atmospheric Δproxy/ΔffCO$_2$ ratios found in the three individual campaigns are presented and, where possible, compared with TNO and other emission inventories.

VERIFY is a research project funded by the European Commission under the H2020 program. Grant Agreement number 776810.

4. Previous proxy/ffCO$_2$ studies

In the literature, several studies investigating proxy/ffCO$_2$ can be found. The majority of the studies focused on the CO/ffCO$_2$ ratio as the lifetime of CO is long compared to diurnal and synoptic time scales. Different experimental approaches and study designs were used, ranging from aircraft-based observations to ground-based urban atmospheric stations to dedicated studies mapping a specific source sector. The latter type of studies is most relevant to us, while we will not discuss airborne and station-based results in our context. Table 4.1 compiles the reported $\Delta CO/\Delta CO_2$ and $\Delta NO_x/\Delta CO_2$ ratios[1], respectively. We are not aware of any proxy/ffCO$_2$ study focusing explicitly on the residential sector. Thus, the discussed examples are for the traffic sector only.

Table 1 Literature results on Δproxy/ΔCO$_2$ emission ratios from the traffic sector.

Publication	**ΔCO/ΔCO$_2$ (ppb/ppm)**	**measurement type**
Bishop et al., 2007	9 to 18	traffic — tailpipe
Vollmer et al., 2007	9.2 ± 3.7	traffic — tunnel
Vollmer et al., 2014	4.15 ± 0.34	traffic — tunnel
Ammoura et al. 2014	8.44 ± 0.45	traffic — tunnel
	ΔNO$_x$/ΔCO$_2$ (ppb/ppm)	**measurement type**
Ammoura et al 2014	4.42 ± 0.25	traffic — tunnel

While Bishop and Stedman [2008] and Vollmer and co-workers [2007, 2014] report $\Delta CO/\Delta CO_2$ ratios only, Ammoura and co-workers [2014] report both $\Delta CO/\Delta CO_2$ and $\Delta NO_x/\Delta CO_2$ ratios. The tailpipe observations of Bishop et al. showed a large variability of 8 to 18 ppb/ppm for individual cars. Vollmer et al. conducted a tunnel study near Zurich and found mean $\Delta CO/\Delta CO_2$ ratios for the Swiss car fleet of 9 ppb/ppm in 2004/2005, which reduced to 4 ppb/ppm in 2011. The reduction of the $\Delta CO/\Delta ffCO_2$ ratio with time was expected, as the combustion efficiency of cars was expected to increase. In a highway tunnel study in Paris, Ammoura et al. (2014) found average $\Delta CO/\Delta CO_2$ ratios of 8.44 ± 0.45 ppb/ppm and $\Delta NO_x/\Delta CO_2$ of 4.42 ppb/ppm for the year 2012.

[1]Both study designs, tailpipe and tunnel setups measure the total CO_2 signal which is dominated by the traffic emissions. A small difference between ΔCO_2 and $\Delta ffCO_2$ exists as gasoline and diesel can contain an admixture of biofuels. We account for this when comparing the reported $\Delta proxy/\Delta CO_2$ ratios to the TNO ratios. The difference between TNO proxy/CO2 and proxy/ffCO$_2$ ratio is 5% for Paris 2012 and less than 1% for all other cases.

VERIFY is a research project funded by the European Commission under the H2020 program. Grant Agreement number 776810.

Table 4.2 summarises the comparison between the three tunnel studies and the TNO proxy/CO_2 ratios for the relevant year and regions. In both studies by Vollmer et al., measured $\Delta CO/\Delta CO_2$ ratios are smaller (by a factor of 2 and 3 for the years 2004 and 2011, respectively) than the CO/CO_2 ratio given by TNO. The study of Ammoura et al. agrees well with TNO in both $\Delta CO/\Delta CO_2$ and $\Delta NO_x/\Delta CO_2$.

Table 4.2: Comparison of different studies with TNO traffic data for the corresponding year and region. The regions are: Zurich, 8.35-8.70 °E and 47.3-47.55°N; Paris, 2.1-2.7°E and 48.7-49.0°N. The spatial area in the TNO inventory was estimated to include the whole city plus smaller towns nearby. TNO emission ratios account for biofuel emissions' of the traffic sector (between 1 – 5%).

study	study year	$\Delta CO/\Delta CO_2$ (ppb/ppm)	$\Delta NO_x/\Delta CO_2$ (ppb/ppm)	TNO year	TNO region	CO/CO_2 (ppb/ppm)	NO_x/CO_2 (ppb/ppm)
Vollmer et al. 2007	2004	9.2	--	2005	Zurich	19.13	3.08..4.72
Vollmer et al. 2014	2011	4.15	--	2011	Zurich	12.27	2.39..3.67
Ammoura et al. 2014	2012	8.44	4.42	2012	Paris	s8.19	3.79..5.81

Although both tunnel studies (Paris and Zurich) were carried out for highway, or highway-like situations in 2011 and 2012, the observed $\Delta CO/\Delta CO_2$ ratios differed by a factor of 2, with Paris having the higher ratio. At the same time, the inventory-predicted CO/CO_2 emission ratios are 50% higher for Zurich. A country dependent fleet composition can explain the difference in the inventory-based proxy/CO_2 ratios. In 2019, the ratio of petrol to diesel cars in Switzerland was about 50:50, whereas, in France, it was about 25:75 [personal communication: Hugo Denier van der Gon, 2021]. Diesel cars emit less CO and more NO_x.

The mismatch between TNO and the Zurich studies is attributed to the changing emission ratio depending on the driving cycle. For highway situations with fluent traffic, the CO/CO_2 emission ratios are reduced up to a factor of 2 while there is only a minor change in the NO_x/CO_2 ratio [personal communication: Hugo Denier van der Gon, 2021]. On the other hand, Ko et al. [Ko et al., 2018] showed that the CO/CO_2 emissions are reaching emission ratios of 43 ppb/ppm during the cold start phase.

To summarise the literature's results, we have to conclude that there is no single proxy/CO_2 ratio for the traffic sector. The driving cycle and fleet composition are essential variables that have to be considered when determining the proxy/ffCO_2 ratio of the traffic sector. State-of-the-art emission inventories, like the TNO inventory, are accounting for fleet composition and driving conditions by applying different proxy/ffCO_2 ratios. Therefore, the experimental Δproxy/ΔffCO_2 study aims to evaluate the proxy/ffCO_2 for a given fleet composition and driving situation with respect to the TNO inventory.

VERIFY is a research project funded by the European Commission under the H2020 program. Grant Agreement number 776810.

5. Experimental approach and instrumentation

In the following, we describe the experimental approaches to determine source sector dominated Δproxy/ΔffCO$_2$ ratios and introduce the instrumentation applied during the campaigns.

5.1. Experimental approaches

The rationale for investigating effective atmospheric Δproxy/ΔffCO$_2$ ratios is based on the following considerations:

a) The proxy/ffCO$_2$ ratios of individual emitters, such as individual cars or heating systems, are variable and depend on specific conditions such as, e.g. combustion temperature, operating duration and others. Direct atmospheric measurements have the advantage of integrating over many emitters and thus, reflect an emission weighted effective atmospheric ratio for the respective source type.
b) The NO$_x$ concentration, in particular, is subject to photochemical reactions. Therefore, in-situ observation of the Δproxy/ΔffCO$_2$ ratio under natural photochemical conditions are desirable in addition to direct exhaust pipe measurements.

This study targets the effective atmospheric Δproxy/ΔffCO$_2$ ratios for the traffic and the residential heating sector since, firstly, both sectors significantly contribute to the total ffCO$_2$ emissions in urban areas. Secondly, both sectors are less specific than individual point sources. We applied the following two sampling approaches:

- Two-station approach
  The two-station approach uses paired observations upwind and downwind of the sources of interest. If both stations are aligned on one trajectory, the observed concentration enhancements are predominantly caused by the emissions between both stations. The upwind station is the “background” measurements, whereas the downwind station is the so-called “signal” measurements. We applied the two-station approach for determining the Δproxy/ΔffCO$_2$ emissions from highway traffic emissions for the in-situ (Sec. 5.2) and the total column observations (Sec. 5.3).

- Single-station approach
  The single-station approach uses one station and exploits the information contained in the temporal concentration changes. Well-mixed atmospheric conditions are used to define the “background” concentration levels for all investigated gas species. During atmospheric inversion conditions, the concentration build-up in the lower boundary layer relates to emissions in the near field of the station. Flasks sampled during inversion situations are further referred to as “signal” flasks. This approach integrates over a specific footprint area and applies to emissions from distributed sources such as the residential heating sector. Using the lowermost atmosphere layer as integrating volume goes hand in

VERIFY is a research project funded by the European Commission under the H2020 program. Grant Agreement number 776810.

hand with the unavoidable problem that also other sources contribute to the observed Δproxy/ΔffCO$_2$ ratios. We try to minimise this effect by first choosing a location where there are few non-target sources and secondly by investigating certain times when non-target sources contribute less.

Determining the absolute ffCO$_2$ enhancement is essential in both approaches. However, this is only possible for in-situ campaigns. For the total column measurements, the ΔXCO$_2$ needs to be used instead. The in-situ campaigns use ^{14}C-based fossil fuel CO$_2$ estimates, which rely on differential ^{14}CO$_2$ measurements between the "background" and the "signal" situation or location according to Eq. 1 adopted from Levin et al. (2008):

$$\Delta \mathrm{ff}CO_2 = \frac{\mathrm{CO}_{2,\mathrm{bg}}(\Delta^{14}C_{\mathrm{bg}} - \Delta^{14}C_{\mathrm{bg\,nuc}} - \Delta^{14}C_{\mathrm{bio}}) - \mathrm{CO}_{2,\mathrm{sig}}(\Delta^{14}C_{\mathrm{sig}} - \Delta^{14}C_{\mathrm{sig\,nuc}} - \Delta^{14}C_{\mathrm{bio}})}{\Delta^{14}C_{\mathrm{bio}} + 1000\ ‰}, \quad (1)$$

where CO$_{2,x}$ and $\Delta^{14}C_x$ are the measured CO$_2$ concentration and its corresponding radiocarbon ^{14}C/C ratio expressed in Δ notation according to Stuvier and Polach (1977), for either the background (bg) or the signal (sig). $\Delta^{14}C_{x\,nuc}$ accounts for the ^{14}CO$_2$ contamination from nuclear facilities, $\Delta^{14}C_{bio}$ is the Δ^{14}C signature of the biogenic respiration flux.

Both ffCO$_2$ proxies, CO and NO$_x$, are measured continuously. In addition, the ICOS Flask and Calibration Laboratory (FCL) in Jena, Germany, measured the CO$_2$ and CO concentration for each flask sample. We use the flask measurements to calculate the CO enhancements (ΔCO) (signal - background). The short photochemical lifetime of NO$_x$ prevents offline measurements; thus, we calculate the NO$_x$ enhancement (ΔNO$_x$) (signal - background) from the in-situ measurements over the flask sampling period, typically being one hour. These proxy enhancements and the ΔffCO$_2$ are used to derive the effective atmospheric Δproxy/ΔffCO$_2$ ratios. The Δproxy/ΔffCO$_2$ ratio uncertainties are calculated by error propagation of the 1σ measurement uncertainties of CO, NO$_x$, CO$_2$ and ^{14}CO$_2$. For calculating the mean Δproxy/ΔffCO$_2$ ratios, individual ratios are inversely weighted with their assigned measurement uncertainty:

$w_i = 1/\Delta_i^2$,

where Δ_i is the error of ratio *i* and w_i is the corresponding weight[2]. The weighted standard deviation is calculated according to [Rukhin 2009][3].

[2] Weights are chosen based on the maximum likelihood approximation method described in Rukhin (2009), formula: https://www.itl.nist.gov/div898/software/dataplot/refman2/ch2/weigmean.pdf
[3] the formula can be found here: https://www.itl.nist.gov/div898/software/dataplot/refman2/ch2/weightsd.pdf

VERIFY is a research project funded by the European Commission under the H2020 program. Grant Agreement number 776810.

5.2. Mobile in-situ laboratories

For the in-situ measurements, two mobile laboratories were designed by UHEI and built by the associated workshop of the Institute of Environmental Physics. The laboratories are built in a temperature isolated box trailer (3.06 m x 1.75 m x 1.90 m (L x W x H)) shown in Figure 5.1. An air conditioning unit ensures constant temperatures improving the repeatability of the in-situ instrumentation in the mobile laboratories. The intake lines for the in-situ measurements are connected to an extendable 10 m mast.

Figure 1: Mobile Laboratory 1 in Leimen.

Both mobile laboratories are equipped with instrumentation to measure in-situ concentrations of CO_2, CO, and NO_x. Each mobile laboratory contains an automated flask sampler to allow for $^{14}CO_2$ analysis. Mobile Laboratory One (short: ML1) is equipped with a weather station and a Heidelberg Radon-monitor [Levin et al., 2002] in addition.

^{222}Rn, a progeny of ^{238}U, is a noble gas and exhaled from soils at a rate of in the order of 1 atom per cm^2/s, depending on soil texture, local water table depth and uranium content [Karstens et al., 2015]. ^{222}Rn is used as a tracer for local atmospheric transport and mixing [Dörr et al. 1986] and thus of particular importance for the single station approach. In the two-station approach, only the trace gases and the flask have to be measured or sampled at both locations. Since the two stations have been less than 1 km apart, it is sufficient to measure ^{222}Rn and the meteorological parameters only at one station.

It is vital for the two-station approach that the trace gas measurements in both mobile laboratories are compatible. We equipped both mobile laboratories with three calibrated gas cylinders provided by the ICOS FCL in Jena, which span an appropriate CO_2 and CO concentration range. Two calibrated cylinders have been used to calibrate the CO_2 and CO instruments in each laboratory, while the third cylinder acted as quality control gas. The NO_x instrument (ICAD) does not need calibration with gas cylinders since it is based on its measurement principles. The ICAD instruments only require path length calibration, which is done by purging the cavity with zero air, i.e., air from which NO_x is removed by an active charcoal filter and humidity is reduced by silica gel [Horbanski et al., 2019].

VERIFY is a research project funded by the European Commission under the H2020 program. Grant Agreement number 776810.

5.3. Mobile total-column instrumentation

A pair of identical mobile ground-based FTIR spectrometers were deployed for the total-column measurements. Physically, the instruments are identical in construction to the one shown in Figure 5.2. The commercial designation used by the manufacturer Bruker is EM27/SUN. These instruments offer the possibility of quantifying column-averaged abundances of several trace gases, among these the most essential GHGs (CO_2, CH_4) and CO from solar absorption spectra with the advantage of being portable, easy to set up and considerably cheaper than the high-resolution instruments used by the TCCON network (Bruker IFS 125HR). Most notably, the spectrometer maintains its calibration over long time scales (several years), also unaffected by relocating the instruments during the campaign [Frey et al., 2019]. Gisi et al. [2012] and Hase et al. [2016] described the spectrometer's design and performance.

Figure 5.2: EM27/SUN spectrometer during field deployment for the VERIFY highway campaign. The spectrometer is covered under a sunshade for avoiding heating of the electronics by solar insulation.

The precision of the column-averaged abundances depends on the integration time applied. Generally, COCCON recommends to co-add ten double-sided interferograms recorded at 10 kHz sampling rate. This results in an integration time of one minute per measurement. A spectrum is calculated and subsequently analysed for deriving the atmospheric trace gas contents from the co-added interferograms. Typically, a precision (1σ empirical standard deviation) of 0.1 ppm for XCO_2, 0.3 ppb XCH_4, and 0.2 ppb for XCO is achieved under clear-sky conditions. Using Allan variance analysis to the measured column difference for co-located instruments, the precision of differential column measurements was estimated by Chen and co-workers to be in the range of 0.01 [Chen et al., 2016] for XCO_2 and XCH_4, a result even more favourable than the previous estimates.

VERIFY is a research project funded by the European Commission under the H2020 program. Grant Agreement number 776810.

6. Campaigns

Despite the highly adverse framework conditions imposed by the COVID-19 pandemic, the planned field campaigns were conducted successfully. The only modification to the initial planning was that the combined (in-situ + total column) traffic campaign had to be split into two individual campaigns (described in Sec. 6.2 and Sec. 6.3).

6.1. Residential heating sector (UHEI)

The first campaign targeted the emission ratios of the heating sector. For this, we applied the single-station approach in a residential area.

6.1.1. Heating campaign setup and site descriptions

We conducted the residential heating campaign in Leimen, Germany (lat. 49.352 °N, long. 8.6913 °E, alt: 138 m asl) from Mar 27th to Apr 2nd 2020. Leimen is located on the east edge of the Upper Rhine Valley, partially elevated by the offshoots of the Odenwald (a mountain ridge confining the Upper Rhine Valley).

Figure 6.2 Leimen. Pin "mobile laboratory" marks the position of the mobile laboratory during sampling.

Figure 6.1 shows an aerial image (Google Earth) of the measurement site located at the end of a dead-end road to avoid emissions from transit traffic. The next more significant road is located in a westerly direction at a distance of 150 m. The houses in the immediate vicinity comprise different heating systems using different fuels. The nearest five houses use oil-fuelled heating systems. Further to the South, oil- and gas-fuelled heating systems are supported by wood-fuelled tiled and fireplace stoves. To the best of our knowledge, no coal-fired heating systems do exist in Leimen. A cement plant is located 635 m North of the sampling site. Due to the 87 m high chimney, the local measurements are not strongly influenced by the cement plant emissions. The potential influence of this plant will be discussed in the results section.

Although the timing of the campaign was quite late in the seasonal heating period, the average temperature was 5.4 °C with typical night time (18:00 - 06:00) temperatures of 0 °C to 5 °C (mean

VERIFY is a research project funded by the European Commission under the H2020 program. Grant Agreement number 776810.

3.1 °C) and daytime (06:00 - 18:00) temperatures of up to 12.5 °C (mean 7.6 °C). The actual temperatures measured during the campaign are given in Figure 6.2 in the lowest panel.

We applied the single-station approach for the residential heating campaign using the fully equipped Mobile Laboratory 1 (ML1). Residential heating emissions have seasonally changing diurnal patterns, depending on ambient temperature and human behaviour [Gadd and Werner, 2013]. Especially during the shoulder seasons where the campaign took place, the nocturnal heat demand is relatively constant and at its diurnal minimum, but the heating systems still operate at baseload conditions. The heat demand increases 4-6-fold in the early morning hours between 04:00 and 06:00 local time. This peak in heat demand is due to the consumption of hot water and the heating of living areas at the beginning of the daily human routine [Heitkoetter et al., 2020]. Depending on the type of heating systems, ambient temperatures and individual human behaviour, the heating demand during the day is 1-3-fold the nocturnal demand. In the evening hours between 17:00 and 22:00, the second smaller and much broader heating demand peak occurs with about 2-4 times the nocturnal demand [Heitkoetter et al., 2020].

Thus, the diurnal cycle of the ffCO_2 emissions from the residential heating sector is different compared to the one of traffic or industry. Traffic emissions are directly linked to human movement and thus minimal during night, even lower than residential emissions operating in baseload conditions. Traffic emissions typically start at 05:00 and strongly peak during 06:00 and 08:00 local time. High traffic emission persists throughout the day with a smaller and broader peak in the evenings between 16:00 and 19:00. After that, the traffic emissions are decreasing towards their nocturnal minimum.

To maximise the influence of the residential heating sector when applying the single-station approach, we focus on the observations during the nocturnal build-up before the strong traffic emissions in the morning start. According to the diurnal cycles of traffic and residential heating, the strongest heating imprint can be expected between 04:00 and 05:00 when the heating systems started, but the traffic is still very limited.

Table 6.1 shows the instruments used for the heating campaign, including reproducibilities and time resolutions. While the performance of the Picarro G2301 was stable, the Aerolaser 5001 showed stability issues: Throughout the whole campaign, the sensitivity fell off by 12.5%, and the instrument temperature was unstable.

VERIFY is a research project funded by the European Commission under the H2020 program. Grant Agreement number 776810.

Table 6.1 Instruments used in Mobile Laboratory 1 for the residential heating sector campaign. Reproducibilities are based on target cylinder measurements: the offset to the calibrated value and the standard deviation of the measurements are given.

use period	instrument	function	reproducibility	time res.
whole heating campaign	Picarro G2301	CO_2 and CH_4 measurement	CO_2: -0.03 ± 0.51 ppm	1s, averaged to minutes
whole heating campaign	Aerolaser 5001	CO measurements	CO: -1.01 ± 8.49 ppb	1s, averaged to minutes
whole heating campaign	Flask Sampler	collect air samples	—	—
whole heating campaign	Heidelberg Radon Monitor	^{222}Rn, ^{214}Po measurement	—	30 min
whole heating campaign	Thies weather station	wind speed, wind direction, temperature	—	1s, averaged to minutes

6.1.2. Heating campaign results

Twenty flasks were sampled during the heating campaign and subsequently analysed for $^{14}CO_2$ to derive ffCO_2 estimates. The proxies concentrations, CO and NO_x, were measured continuously as described in Sec. 5.1.

Figure 6.2 gives an overview of the continuous in-situ measurements from 30/03/2020 06:00 to 02/04/2020 04:00[4]. The first four panels show CO_2, CO, NO_x (NO_x in red, NO_2 in blue), and ^{222}Rn concentrations. The lower three panels show the meteorological parameters wind speed, wind direction and temperature. Vertically shaded bars depict flask sampling times. Each flask sample is numbered in the order of appearance, starting with number 3. We screened the three-day observation period for background conditions applying the following two criteria: low ^{222}Rn concentrations and moderate wind speeds. Samples 3, 8 and 9 fulfil these criteria. Table 6.2 summarises the concentrations as well as the isotopic composition for those three background flasks. Although the flasks were taken on different days and at different times of the day, they all show a remarkable agreement between their concentrations. We conclude that this is a representative estimate of the background concentrations that occur when the locally polluted air is removed and replaced by fresh air. Thus, the average of these three events is used as background concentration for the individual species for the remaining evaluation.

[4] Measurements stopped abruptly due to electrical failure of the instrument drying the air for the other instruments.

VERIFY is a research project funded by the European Commission under the H2020 program. Grant Agreement number 776810.

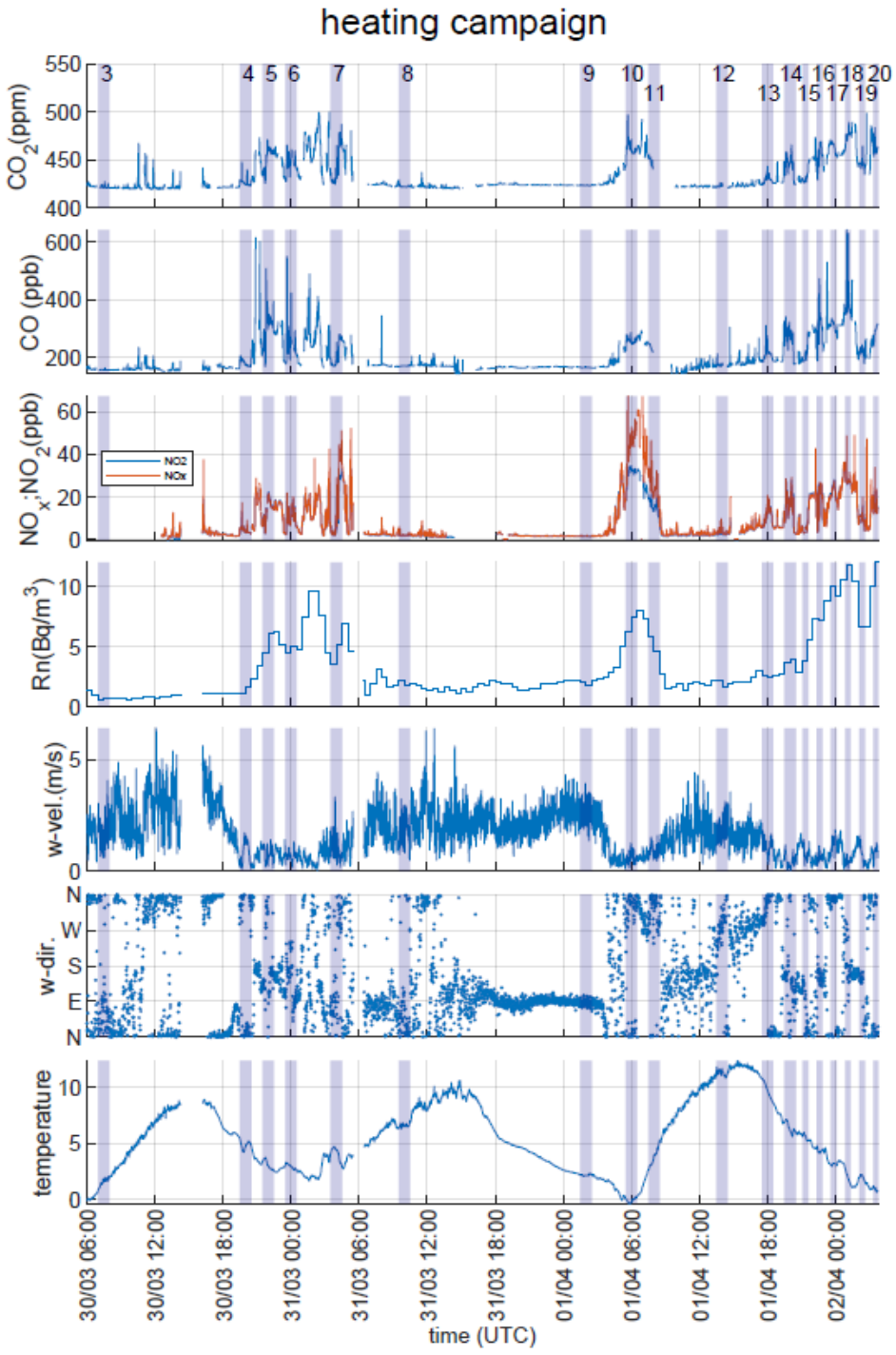

Figure 6.2: Overview of the continuous in-situ measurements for the heating campaign. The first four panels show CO_2, CO, NO_x (NO_x in red, NO_2 in blue), and ^{222}Rn concentrations. The lower three panels show the meteorological parameters wind speed, wind direction and temperature. Vertically shaded bars depict flask sampling times.

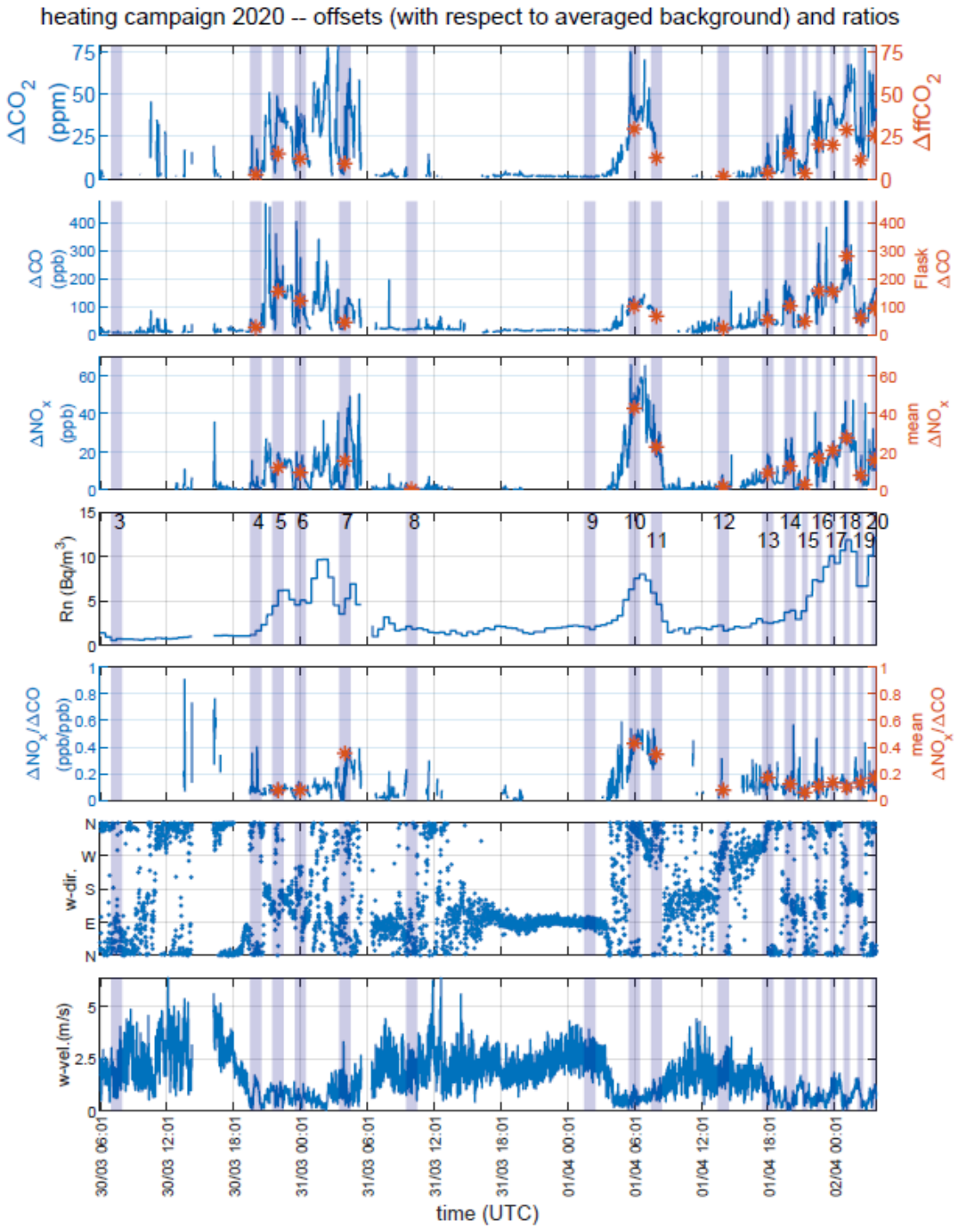
heating campaign 2020 -- offsets (with respect to averaged background) and ratios
ΔCO2 (ppm)
ΔffCO2
ΔCO (ppb)
Flask ΔCO
ΔNOx (ppb)
mean ΔNOx
Rn (Bq/m3)
ΔNOx/ΔCO (ppb/ppb)
mean ΔNOx/ΔCO
w-dir.
w-vel.(m/s)
3 4 5 6 7 8 9 10 11 12 13 14 15 16 17 18 19 20
30/03 06:01
30/03 12:01
30/03 18:01
31/03 00:01
31/03 06:01
31/03 12:01
31/03 18:01
01/04 00:01
01/04 06:01
01/04 12:01
01/04 18:01
02/04 00:01
time (UTC)

Figure 3

The first three panels of Figure 6.3 show the continuously measured local trace gas enhancements (ΔCO_2, ΔCO and ΔNO_x) with respect to the average background concentrations. The red stars show enhancements for the flask sampling time according to the right axis. In the ΔCO_2 panel, the $^{14}CO_2$-based $\Delta ffCO_2$ estimates are shown. In the ΔCO panel, the red stars are derived from the flask measurements providing independent quality control for the in-situ measurements, while in the ΔNO_x panel, the red stars give the averaged ΔNO_x value for the flask sampling period. The fourth panel shows the $\Delta NO_x/\Delta CO$ ratio of the in-situ data and the flask data. As for any ratio of atmospheric trace gases, the transport-related variability observed in the individual enhancements cancels for the ratio as both tracers are subject to the same atmospheric transport. The last three panels show ^{222}Rn, wind speed and direction, similar to Figure 6.2, to indicate atmospheric conditions.

Table 6.2 Background samples and the averaged background.

date	CO_2 (ppm)	$CO_{2,Err}$ (ppm)	CO (ppb)	CO_{Err} (ppb)	NO_x (ppb)	$NO_{x,Err}$ (ppb)	Rn (Bq/m^3)	$\Delta^{14}C$ (‰)	$\Delta^{14}C_{Err}$ (‰)	$\delta^{13}C$ (‰)	$\delta^{13}C_{Err}$ (‰)
30.03.2020 07:00	421.35	0.04	143.9	5.17	NaN	NaN	0.62	-7.52	2.24	-9.15	0.03
31.03.2020 09:30	421.88	0.04	153.13	1.01	2.12	0.09	1.97	-8.58	2.24	-9.24	0.02
01.04.2020 01:30	422.57	0.04	150.74	0.47	1.42	0.02	1.91	-9.06	2.27	-9.44	0.01
mean	421.93	0.04	149.26	3.05	1.77	0.05	1.50	-8.38	2.25	-9.28	0.03

Looking at the ^{222}Rn concentrations in Figure 6.2, we can identify three events with a reduced atmospheric mixing:

Event I from 30.03. 18:00 to 31.03. 06:00 UTC

Event II from 01.04. 03:00 to 01.04. 09:00 UTC

Event III from 01.04. 18:00 to 02.04. 04:00 UTC

Low wind speeds and accumulating trace gas concentrations characterise all events. The temporal variations of ΔCO_2, ΔCO and ΔNO_x, are strongly correlated throughout the entire period. After discussing each event in more detail, we will evaluate all flask samples for their $\Delta proxy/\Delta ffCO_2$ ratios.

During Event I (30.03. 18:00 to 31.03. 06:00), the CO_2, CO, and NO_x enhancements fluctuate strongly, nearly going down to background levels. Joint interpretation of wind conditions and CO_2 enhancements (not shown here) showed that enhanced wind speeds and northerly directions are correlated with lower ΔCO_2, while high ΔCO_2 was dominant at low wind speeds. Also, the ^{222}Rn build-up is interrupted before samples #6 and #7. We interpret this as flushes of “fresh” air. As the individual concentration build-ups occur during low wind speeds, we conclude that we

VERIFY is a research project funded by the European Commission under the H2020 program. Grant Agreement number 776810.

measured local source emissions during this event. Sample #7 was collected at the end of the event at 04:00 UTC (06:00 local time), and the $\Delta NO_x/\Delta CO$ ratio of #7 is three times higher than the earlier samples. Due to the timing, a mix between heating and traffic emissions can be expected and thus, sample #7 will be excluded.

Event II (01.04. 03:00 to 01.04. 09:00) is different from Event I. In Figure 6.2, we find only for Event II a split between NO_x and NO_2, i.e., the NO_x signal contains NO. In Figure 6.3 shown that the $\Delta NO_x/\Delta CO$ ratio changes significantly during this event and is three to four times the ratio observed during Event I. The build-up of Event II started around 04:00 UTC (06:00 local time). The first flask was sampled between 06:00 and 07:00 UTC. Similar to sample #7, samples #10 and #11 are excluded when determining the average heating emission ratios.

Event III (01.04. 18:00 to 02.04. 04:00 UTC) shows similarities to Event I. In the beginning, we see a gentle ^{222}Rn build-up which is accelerating after 22:00 local time. Around 04:00, the decrease in ^{222}Rn indicates a contribution of "fresh" air. Combing wind and ΔCO_2 data confirms the earlier finding that larger ΔCO_2 go along with lower wind speeds. Apart from sample #13 taken at 18:00 UTC (20:00 local time), which still may contain traffic emission contribution, the remaining samples #14 to #20 have been sampled during conditions where the residential heating emissions dominate.

Apart from the flasks sampled during background conditions (#3, #8 and #9), only flask #12 was not sampled during one of three events. Flask #12 was taken at 08:00 UTC (10:00 local time) and is thus not suited for determining the heating ratios.

VERIFY is a research project funded by the European Commission under the H2020 program. Grant Agreement number 776810.

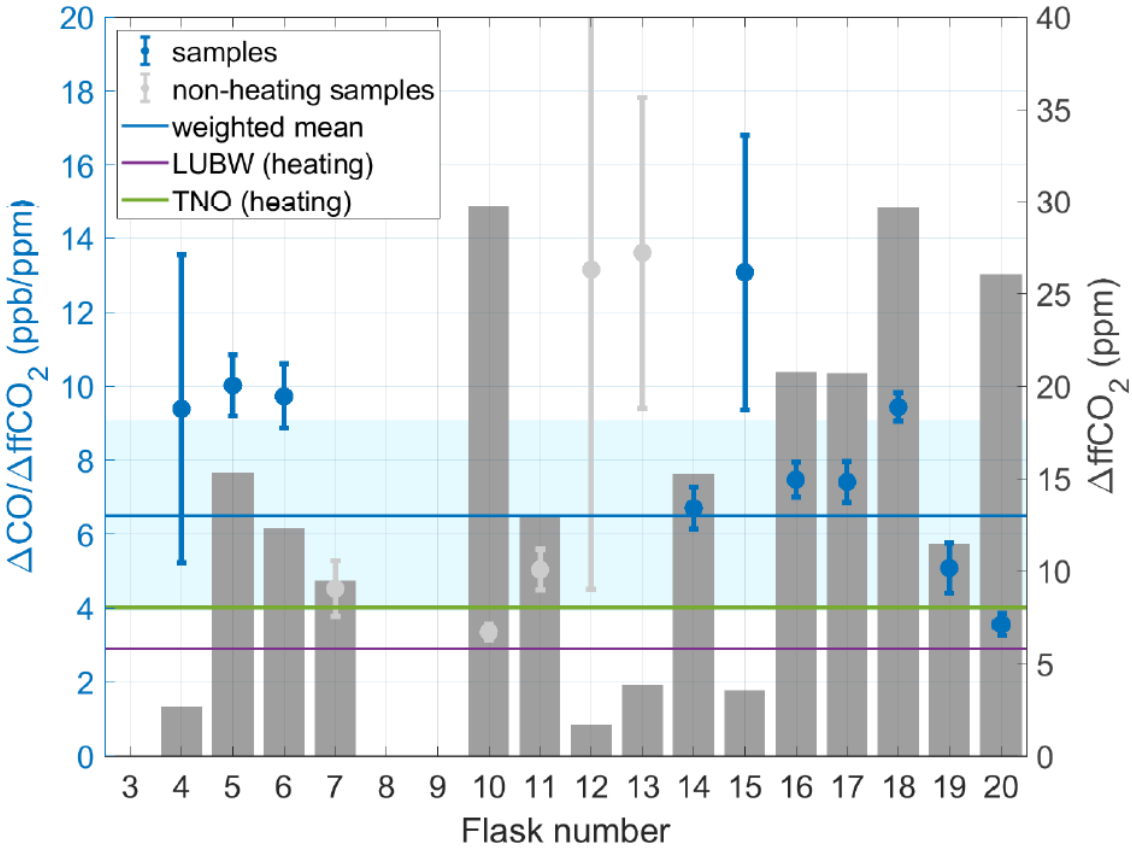

Figure 6.4 Effective atmospheric ΔCO/ΔffCO$_2$ ratios for heating dominated (blue dots) and mixed situations (gray dots) referring to the left axis. ffCO$_2$ enhancements are shown as bar charts (right axis). The weighted average for all heating dominated ratios is given by the blue line together with the weighted standard deviation as blue shaded area. Different inventory-based CO/ffCO$_2$ heating emission ratios from TNO and LUBW are plotted as horizontal lines for comparison.

An overview of the effective atmospheric Δproxy/ΔffCO$_2$ ratios is given in Figures 6.4 and 6.5. The Δproxy/ΔffCO$_2$ ratios are plotted against the flask number. Flask samples that are not dominated by residential heating emissions are shown as grey symbols. For each sample, the ffCO$_2$ enhancements are plotted as bars with respect to the right y-scale.

The error weighted mean Δproxy/ΔffCO2 ratio is shown as blue line with the weighted standard error given as light blue shading in both plots. The inventory-based ratios for the residential heating are given for TNO (50km x 50km around Heidelberg) in green and for LUBW[5] in purple.

[5] Landesanstalt für Umwelt Baden-Württemberg, https://www.lubw.baden-wuerttemberg.de/. The regional office for environmental issues for the federal state of Baden-Württemberg. Data was provided upon request by Thomas Metzger (Thomas.Metzger@lubw.bwl.de), November 2020.

VERIFY is a research project funded by the European Commission under the H2020 program. Grant Agreement number 776810.

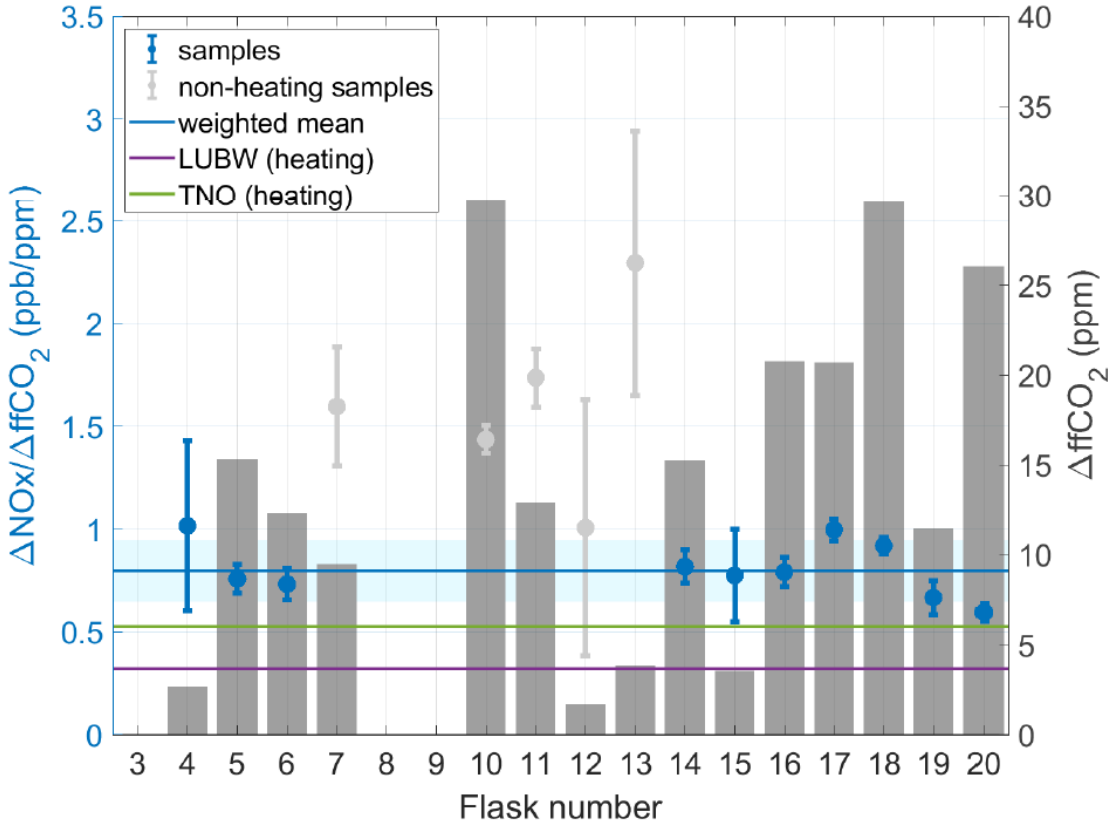

Figure 6.5: Effective atmospheric $\Delta NO_x/\Delta ffCO_2$ ratios for heating dominated (blue dots) and mixed situations (gray dots) referring to the left axis. $ffCO_2$ enhancements are shown as bar charts (right axis). The weighted average for all heating dominated ratios is given by the blue line together with the weighted standard deviation as blue shaded area. Inventory-based $NO_x/ffCO_2$ heating emission ratios from TNO and LUBW are plotted as horizontal lines for comparison.

Especially for the atmospheric $\Delta CO/\Delta ffCO_2$ ratio, we see a large variability. Event I samples (#4-#6) show little spread and a mean $\Delta CO/\Delta ffCO_2$ ratio of 9.7 ppb/ppm. During event III, the ratios change between 3.6 and 13.1 ppb/ppm. The $\Delta NO_x/\Delta ffCO_2$ ratios are more consistent between events I and III and show for both a mean $\Delta NO_x/\Delta ffCO_2$ ratio of 0.80 and 0.84 ppb/ppm, respectively.

The large variability in the $\Delta CO/\Delta ffCO_2$ ratios is not surprising and is be expected due to biofuel consumption (wood and pellets). Biofuels are prone to high CO emissions since combustion conditions (oxygen supply, temperature, etc.) are often not actively optimised and controlled. This is also reflected in the approx. 100 times higher CO emission factor of biofuels compared to oil and gas (EMEP/EEA Guidebook, 2019). Furthermore, biofuels produce no $ffCO_2$ leading to infinite $CO/ffCO_2$ emission ratios. Varying admixtures of biofuels thus leads to significant

VERIFY is a research project funded by the European Commission under the H2020 program. Grant Agreement number 776810.

variations in atmospheric ΔCO/ΔffCO$_2$ ratios, being a major disadvantage when using CO as a proxy for ffCO$_2$ in winter. The NO$_x$ emission factors of biofuels are similar to those of oil and gas (EMEP/EEA Guidebook, 2019) so that the overemphasis of biofuels in the NO$_x$/ffCO$_2$ emission ratios is not reflected to the same extent as in the CO/ffCO$_2$ emission ratios.

Comparing the error-weighted atmospheric mean ratios with inventory-based ratios (Table 6.3 or Figures 6.4 and 6.5), we conclude that the observed Δproxy/ΔffCO$_2$ ratios are higher than both inventories TNO and LUBW. Note that the CO and NO$_x$ emissions from biofuels were always considered when calculating the inventory-based emission ratios. Inventories tend to underestimate biofuel heating emissions [personal communications: Hugo Denier van der Gon and Antoon Visschedijk (TNO)]. The LUBW emission ratios are even lower compared to TNO emission ratios. The local, for Leimen specific, CO/ffCO$_2$ emission ratios of both inventories are a factor of 4 to 2 smaller than the atmospheric observations. The NO$_x$/ffCO$_2$ ratio is underestimated by a factor of 3 to 2. Although these inventory-based ratios should be the most comparable from a spatial point of view, we find that the ratios of the large catchment area (50km x 50km) around Heidelberg fit the observations better. The inventory-based emission ratios for this area underestimate the atmospheric measurements by only about 50%. We, therefore, suspect that the inventory distributes relatively too little biofuel in the smaller towns. Another important observation is that the variability of the TNO emission ratios does not match the atmospheric variability found. The variability of the TNO proxy/ffCO$_2$ emission ratios is based on the results of Super et al. (2020), who varied emission factors and activity data using Monte Carlo simulations. The 40% variability of the atmospheric ΔCO/ΔffCO$_2$ ratio is significantly underestimated in the TNO inventory with 22%. The picture is exactly the opposite for the NO$_x$/ffCO$_2$ ratio. The variation in the atmosphere is only about 20%, but the variability is 130% in the inventory.

Table 6.3 Comparison between the atmospheric mean Δproxy/ΔffCO$_2$ ratios and bottom-up proxy/ffCO$_2$ ratios[6] from two emission inventories and different spatial domains.

	ΔCO/ΔffCO$_2$ (ppb/ppm)	ΔNO$_x$/ΔffCO$_2$ (ppb/ppm)
This study	6.51 ± 2.58	0.80 ± 0.15
inventory	CO/ffCO$_2$ (ppb/ppm)	NO$_x$/ffCO$_2$ (ppb/ppm)
TNO (50 km x 50 km)	4.02 ± 0.88	0.53 ± 0.71
TNO (Leimen)	1.64 ± 0.36	0.43 ± 0.57
LUBW (Leimen)	2.91	0.32

[6] Inventories give emissions as kg/a. Unit conversion with molecular masses was applied. For deducing inventory NO$_x$ emissions, the molecular mass of NO$_2$ (46 g/mol) was used as inventories report NO$_2$ (personal communication with Hugo Denier van der Gon and Antoon Visschedijk).

VERIFY is a research project funded by the European Commission under the H2020 program. Grant Agreement number 776810.

Following the evaluation in the VERIFY Deliverable D2.7, we show the Δproxy/ΔffCO$_2$ ratios in a double ratio plot in Figure 6.6. The samples which have been identified as dominated by the residential heating source are shown in blue. All other samples are shown in grey. As discussed before, the CO/ffCO$_2$ ratio variability can be seen for the heating-dominated samples. For reference, the average emission ratios of industry, power plants and residential heating from TNO (50 km x 50 km around Heidelberg) are shown as well.

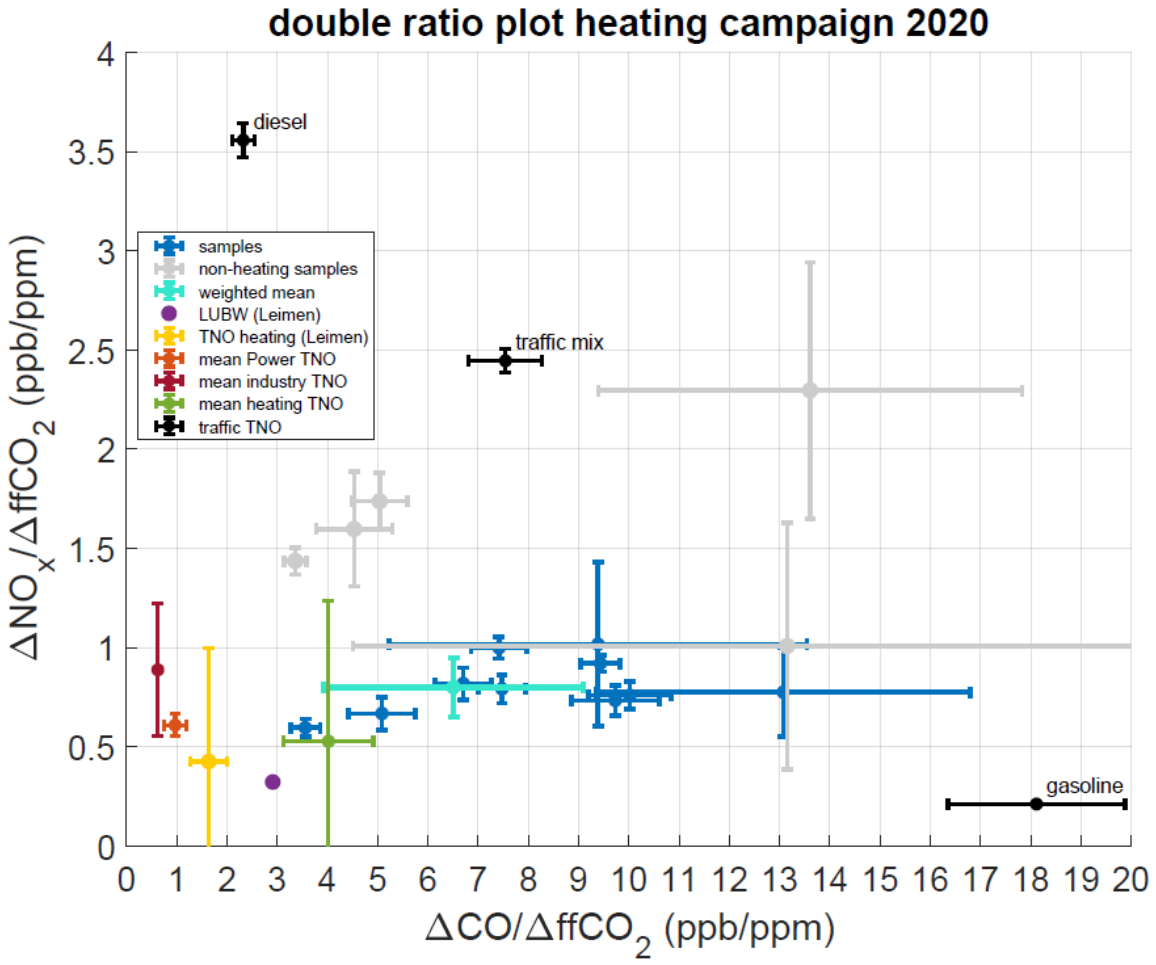

Figure 6.6 Sector-specific double ratios. Samples not used for the weighted average plotted in grey instead of blue. For reference, emission ratios from LUBW (heating, Leimen) and TNO (mean of four sectors in a 50 km x 50 km square around Heidelberg and heating in Leimen) are shown.

VERIFY is a research project funded by the European Commission under the H2020 program. Grant Agreement number 776810.

6.2. Traffic sector (in-situ)

Due to COVID-19 constraints, the start of the in-situ traffic campaign was delayed, and simultaneous total column and in-situ measurements were impossible.

6.2.1. Campaign setup and site description

To study traffic emissions from a highway, the two-station approach using both mobile laboratories was applied. The experimental setup was located in the Rhine Valley to the North West of Heidelberg and targeted highway A5 connecting Frankfurt and Karlsruhe. The highway speed limit at this location is 120 km/h, and there were no construction sites nearby. Data from the traffic agency BASt[7] suggests a below-average truck traffic volume for this highway section. Typical vehicle densities during daytime are between 50 and 100 vehicles per minute. Figure 6.7 shows the location in three levels of detail. The mobile laboratories were in West-East alignment, approximately 800 m apart. The selection of sampling locations had to consider that both laboratories require a wired power supply. The downwind station (ML1) was installed about 20 meters from the centre of the highway. The height difference between the highway and the intake of the downwind station was about 8.5 m.
The instruments used in mobile laboratory 1 (ML1) are listed in Table 6.4, the instruments used in mobile laboratory 2 (ML2) are listed in Table 6.5, each with their corresponding reproducibility. Instrument failure in ML1 forced a change of instruments in November 2020. The campaign was without continuous measurements of CO_2, CO and CH_4 in ML1 until 2020-12-03.

Table 6.4 Instruments used in ML1 for the traffic campaign. Reproducibility is based on QC cylinder measurements: offset ± std dev. to the calibrated values are given.

use period	instrument	function	Reproducibility	time resolution
2020-10-13 to 2020-11-11	Picarro G2301	CO_2 and CH_4 measurement	CO_2: -0.02 ± 0.13 ppm CH_4:-0.2 ± 1.41 ppb	1s, averaged to minutes
2020-10-13 to 2020-11-11	Aerolaser 5001	CO measurements	CO:-15.07±6.18 ppb	1s, averaged to minutes
2020-12-03 to end	Picarro G2401	CO_2, CO and CH_4 measurements	CO_2: -0.06 ± 0.19 ppm CH_4: 0.91 ± 0.57 ppb CO: -2.72 ± 1.44 ppb	1s, averaged to minutes
whole campaign	Flask Sampler	collect air samples	—	—-
whole campaign	Heidelberg Radon Monitor	^{222}Rn, ^{214}Po measurement	—	30 min
whole campaign	Thies weather station	wind speed, wind direction	speed: ± 0.3 m/s direction: ± 2°	1s, averaged to minutes

[7] https://www.bast.de/BASt_2017/DE/Verkehrstechnik/Fachthemen/v2-verkehrszaehlung/Aktuell/zaehl_aktuell_node.html, last called: 20.04.2021

VERIFY is a research project funded by the European Commission under the H2020 program. Grant Agreement number 776810.

Table 6.5: Instruments used in ML2 for the traffic campaign. Reproducibility is based on QC cylinder measurements: offset ± std dev. to the calibrated values are given.

use period	instrument	function	Reproducibility	time resolution
whole campaign	FTIR	CO_2, CO measurements	CO_2: -0.02 ± 0.06 ppm CO:-0.01±0.2 ppb	3 min
whole campaign	Heidelberg Flask Sampler	collect air samples	—	—-

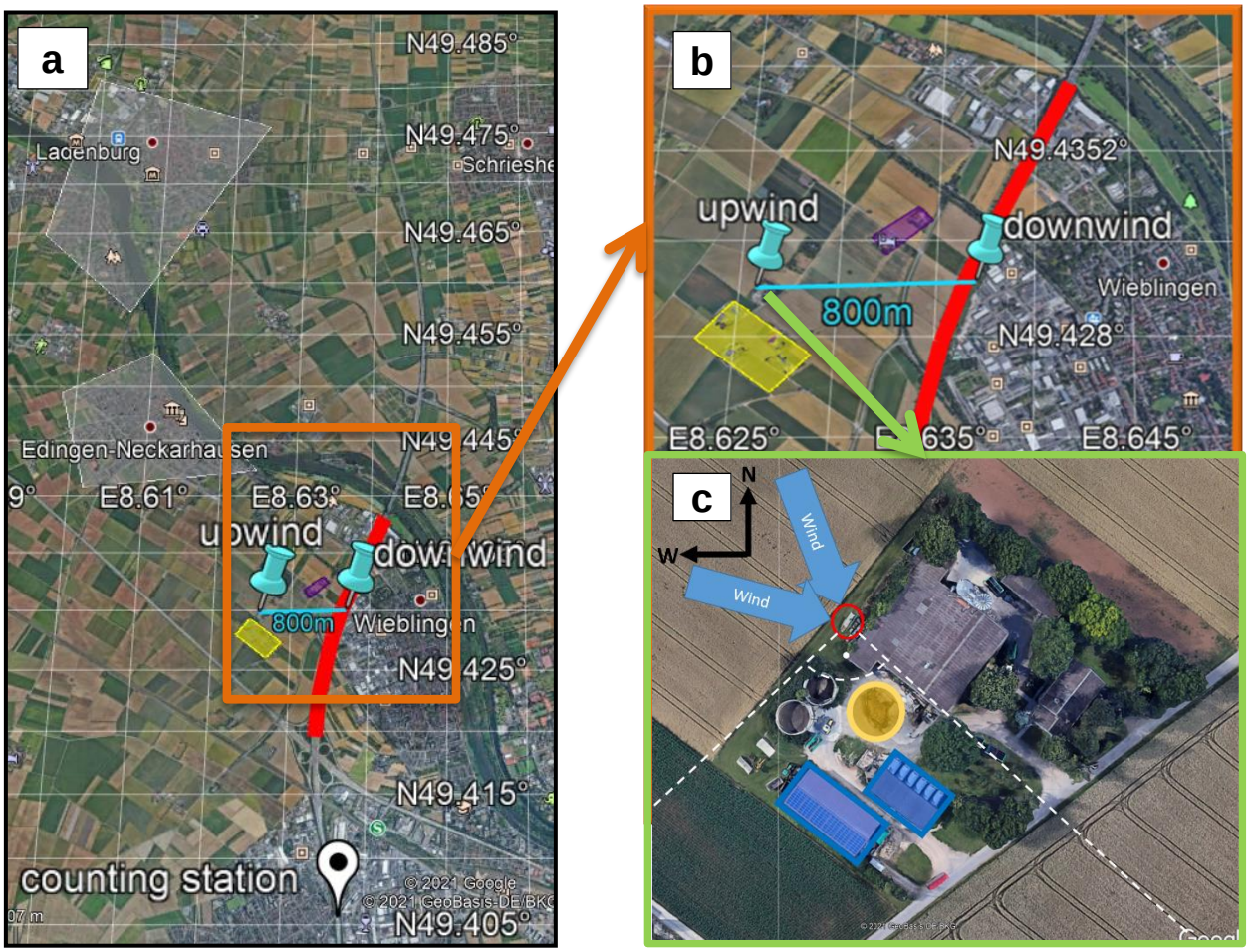

Figure 6.7 Traffic campaign set up. (a) Overview. Mobile laboratories are cyan pins. Highway marked red, counting station Eppelheim is the white pin at the bottom. Grey polygons are close-by towns that are relevant for the same air-mass approach (Edingen-Neckarhausen, Ladenburg). (b) Sampling region. Mobile laboratories are in West-East alignment, 800 m apart, shown here as a cyan line. The yellow rectangle indicates farms near ML2, the upwind station. The purple rectangle indicates two farms 350 m to the North West of ML1, the downwind station. (c) Detailed view of the upwind station. ML2 is circled red, the South quadrant (135° - 225°) is indicated by white dashed lines. Blue rectangles mark animal housings, and the open slurry storage is the yellow circle. Large arrows indicate main wind directions (West, North West).

VERIFY is a research project funded by the European Commission under the H2020 program. Grant Agreement number 776810.

The upwind station was installed on the western boundary of a farm. The farmhouse is located downwind of the upwind station (see Figure 6.7 c). The area enclosed by the two stations comprises the highway, the farmhouse and agricultural fields. In this experimental setting, the highway is the dominant fossil fuel source contributing to the concentration enhancements between the two stations. To estimate the fossil fuel CO_2 influence of the farmhouse on the downwind station, a Gaussian plume model [Turner 1970] was applied. The ffCO_2 emissions of the farmhouse are assumed to correspond to the averaged heating emissions per house in the Heidelberg area calculated based on the TNO emission inventory. We assume that the total residential heating emissions occur during the three winter months and are constant in time. These assumptions result in a mean winter ffCO_2 emission of 1.2 g/s for the farmhouse. Applying the Gaussian plume model, the farmhouse influence on downwind station (ML1) is smaller than 0.02 ppm CO_2 for all daytime atmospheric stability classes applied in [Turner 1970]. The farmhouse influence on the downwind station (ML1) is thus smaller than the measurement precision and much smaller than the observed CO_2 enhancements. Even if the farmhouse emissions would be one order of magnitude higher, the influence would still be negligible.
In order to increase the number of suitable wind conditions for up- and downwind sampling, we applied the so-called “same air-mass” approach. The same air-mass approach assumes well-mixed conditions, i.e. homogeneous trace gas concentrations perpendicular to the wind direction. This assumption is justified if the air mass was previously influenced only by homogeneous surface sources or sinks or if sufficient horizontal mixing occurred after the air mass passed heterogeneous source/sink areas. The question of sufficient horizontal mixing depends not only on the heterogeneity of the source but also on the horizontal distance between the upwind and downwind stations, and a close distance is advantageous. Figure 6.7 b) and c) show the upwind station’s location (ML2) in detail. The farm, including the animal housings and the slurry storage, excludes the southern wind sector from the same air-mass approach. Significant CH_4 emissions partly accompanied by NO_x emissions from the slurry storage and animal housing [Bava et al. 2017] are observed from this southern wind sector. There are no direct buildings to the North and West of both stations. The closest buildings to the downwind station are two farms in 350 m north-western, marked purple in Figure 6.7 b). Both farms do not have livestock. We estimated the influence of the farmhouses ffCO_2 emissions by applying the Gaussian plume model and got a ffCO_2 contribution of smaller than 0.1 ppm for the downwind station (ML1) during the daytime. This is less than 2% of the observed total CO_2 difference between the laboratories.
In the larger catchment area (see Figure 6.7a), two medium-sized towns (Edingen-Neckarhausen: 14 000 inhabitants, Ladenburg: 11 500 inhabitants) are located to the North-West of the setup (at approx. 315° and 330° and a distance of 2.5 km and 4.5 km). TNO emission data suggest comparable ffCO_2, CO and NO_x emissions for the two towns. In the Gaussian plume model, the horizontal dispersion coefficient σ_y at a distance of 2 km is between 150 m and 500 m depending on the atmospheric conditions. At a distance of 5 km, σ_y increases to between 300 m and 800 m. Thus, plumes of point sources in a distance of 2 km cannot be treated as well-mixed across the horizontal distance of both stations. However, in neither of the two towns, significant point sources are present. We, therefore, regard the towns as expanded anthropogenic area sources. The spatial West-East extend of both towns (parallel to the line between ML2 and ML1) is 1.2 km

VERIFY is a research project funded by the European Commission under the H2020 program. Grant Agreement number 776810.

and 2 km, respectively, exceeding the laboratories' distance. The upwind in-situ observations were examined for enhanced concentration during situations when the emission plumes of the cities turn over the station. Neither for CO_2, CO or NO_x a significant concentration enhancement, larger than the typical temporal variability were found[8]. Based on these results, we conclude that the same air-mass approach is applicable to the western and northern catchments. Urban influence can affect the downwind station (ML1) for northerly to easterly wind directions and thus is excluded. In addition, we require that the wind direction varies by less than 20° during the events to ensure more stable conditions during sampling.
In addition to these spatial sample selection criteria, a valid sample must fulfil additional quality criteria. The difference between the in-situ measurement of the mobile laboratories and the offline flask measurement in the ICOS flask and calibration laboratory must not exceed 1 ppm and 5 ppb for CO_2 and CO, respectively. If the two measurement methods diverge further than these thresholds, this indicates that the air sample in the flask may not correspond to the hourly averaged ambient air.

The applied sample selection criteria can be summarised as follows:

(1) Hourly mean wind direction between 260° and 345°
(2) Spread in hourly wind direction less than 20°
(3) difference in CO_2 (in-situ and flask) < 1 ppm
(4) difference in CO (in-situ data and flask data) < 5 ppb

[8] This approach found a CH_4 enhancement for wind directions between 5° and 35°, suggesting a CH_4 point source in this wind direction. This is not relevant for this study but proves the concept of identifying larger point sources by this approach.

VERIFY is a research project funded by the European Commission under the H2020 program. Grant Agreement number 776810.

6.2.2. Results

Figure 6.8 shows a full day of the in-situ traffic campaign measurement from Jan 22nd, 2021. The first four panels give the in-situ CO_2, CO, NO_x, NO_2, and CH_4 concentrations of the downwind station (ML1) and the upwind station (ML2) shown in blue and red. The ^{222}Rn activity concentration, wind speed and wind direction all measured at the downwind station are given in panel 5 to 7, and the traffic load for the Eppelheim counting station[9] are plotted in the lowest panels. Vertical blue shading indicates flask sampling times.

The two-station approach exploits concentration enhancements between down- and upwind stations. Figure 6.9 shows the in-situ CO_2, CO and NO_x concentration enhancements (downwind - upwind) for the example day of Jan, 22nd 2021. The in-situ concentration enhancements refer to the left axis. The ^{14}C-based ffCO_2 enhancement during the flask sampling periods is shown as red stars with respect to the right y-axis in the CO_2 panel. For CO, the red stars show the flask-based CO enhancement, while for NO_x, the red stars are the calculated hourly mean NO_x concentration based on the in-situ data.

We find a good correlation between the CO_2, CO and NO_x enhancements and the traffic volume for wind directions fulfilling the same air-mass approach requirements. The ^{14}C-based ffCO_2 estimates reveal that the major share (>90%) of the CO_2 enhancement is of fossil origin. Due to the addition of biofuels to diesel and petrol, we expect a non-fossil CO_2 contribution from traffic emissions. Measurements by Friedrich and Hammer [2017] show that the average biofuel admixture for diesel and petrol in the Rhine Valley region was 5% in 2017. Considering this, we can conclude that the entire CO_2 enhancement can be attributed to traffic emissions within our measurement precision. Thus, we conclude that the goal of a traffic-dominated experimental setup has been achieved.

[9] Note that between the sampling site and the Eppelheim counting station there is a highway intersection where cars can get on/off the highway. Consequently, the counts at the station in Eppelheim do not represent the exact amount of traffic that is sampled, but give a realistic estimate of traffic activity (location see Figure 6.7).

VERIFY is a research project funded by the European Commission under the H2020 program. Grant Agreement number 776810.

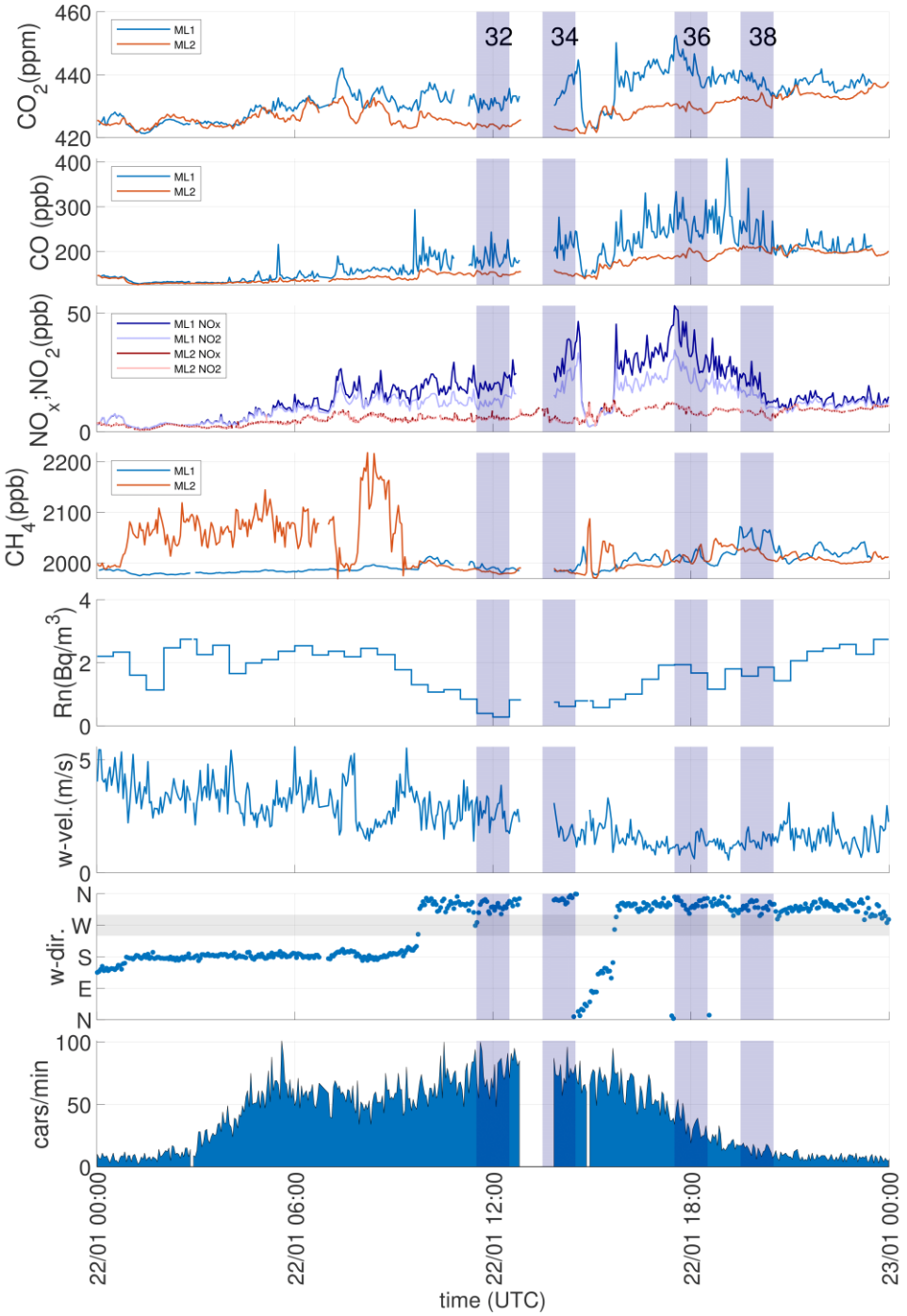

Figure 6.8 Continuous data from upwind (red) and downwind (blue) station on 22/01/2021. Traffic counts according to sampling station Eppelheim. Blue shaded bars are sampling times.

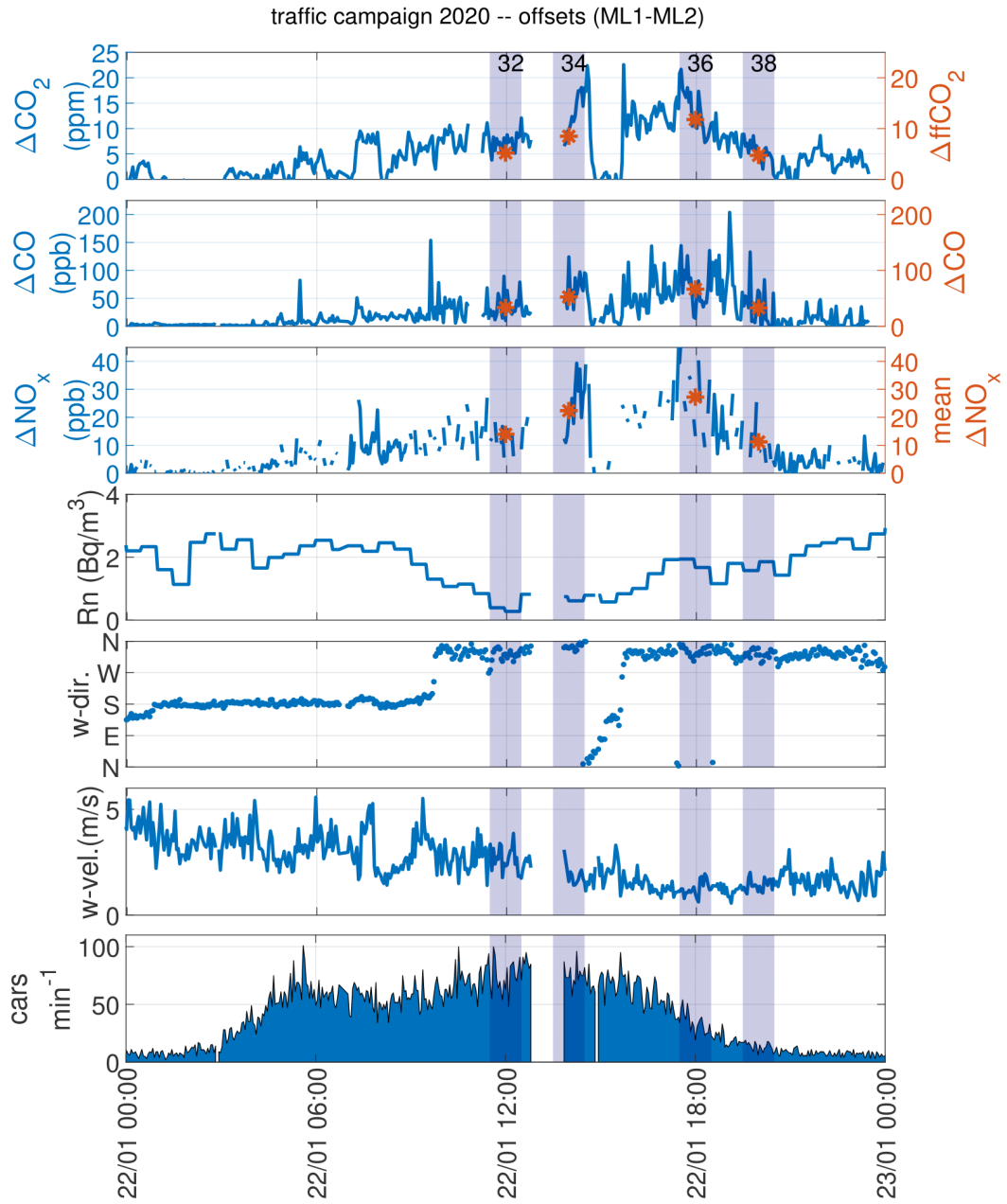

Figure 6.9 CO_2, CO and NO_x concentration enhancements between down- and upwind station on 22/01/2021. The auxiliary parameters (^{222}Rn, and wind) are measured at the downwind station. Traffic counts according to sampling station Eppelheim. Vertical blue shaded areas indicate flask sampling times. Red stars correspond to right axis and show the $ffCO_2$ and CO enhancement based on the flask samples, or indicated the hourly mean NO_x concentrations, respectively.

VERIFY is a research project funded by the European Commission under the H2020 program. Grant Agreement number 776810.

The traffic-specific atmospheric ratios for ΔCO/ΔffCO$_2$ and ΔNO$_x$/ΔffCO$_2$ are determined based on the calculated enhancements. Figure 6.10 shows the emission ratios and their 1σ uncertainties for each flask pair. The absolute ffCO$_2$ enhancement for each flask pair is given as bar chart corresponding to the right axis, ranging between 4.7 and 18.2 ppm. The ^{14}C-based uncertainty of the ffCO$_2$ enhancement of about 1.2 ppm is the most significant uncertainty contribution to the observed atmospheric ratios. Thus, the uncertainty of the observed atmospheric ratio corresponds to the absolute ffCO$_2$ concentration. All observed atmospheric ΔNO$_x$/ΔffCO$_2$ ratios agree within their uncertainties and result in a weighted mean value and 1σ weighted standard deviations of 2.24 ± 0.25 ppb/ppm shown as blue line and blue shaded area in Figure 6.10, respectively. The observed variability in the atmospheric ΔCO/ΔffCO$_2$ is more extensive than for ΔNO$_x$/ΔffCO$_2$, and several ratios do not agree within their uncertainties. The weighted mean and 1σ weighted standard deviations for the ΔCO/ΔffCO$_2$ ratio is 5.21 ± 1.01 ppb/ppm and also shown as blue line and shaded area in Figure 6.10. Both panels of Figure 6.10 show inventory-based proxy/ffCO$_2$ emissions from different inventories or for different emission situations. The LUBW and StaLA[10] inventory estimates represent traffic emissions in the Heidelberg municipality, while the TNO estimates are calculated from traffic emissions in a 50 km x 50 km square with Heidelberg in its centre. The TNO inventory is capable to separately calculate the proxy/ffCO$_2$ emission ratios by different road types [personal communication: Stijn Dellaert, Hugo Denier van der Gon, 21.04.2021]. While the LUBW CO/ffCO$_2$ emission ratio is too high, the StaLA emission ratios fit the observed atmospheric ΔCO/ΔffCO$_2$ ratio. The observed atmospheric ΔCO/ΔffCO$_2$ ratio falls in

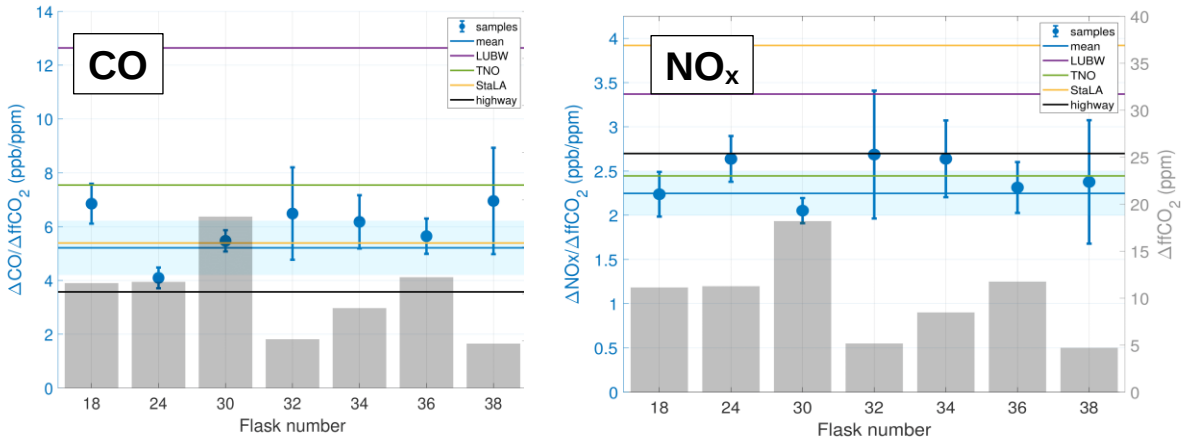

Figure 6.10 Δproxy/ΔffCO$_2$ ratios for valid samples of the traffic campaign. Bottom up inventory estimates of the ratios and the weighted mean ratio (with 1σ weighted standard deviation as blue shaded area) are plotted as horizontal lines. LUBW (purple) and StaLA (yellow) estimates are calculated from traffic emissions for Heidelberg. The green horizontal line represents the TNO estimate calculated from all traffic emissions in a 50 km x 50 km square with Heidelberg in its centre, while the black horizontal line represents the TNO estimate calculated from highway traffic emissions in the same area.

[10] Data provided upon request by Tatjana Kampffmeyer (Tatjana.Kampffmeyer@stala.bwl.de), November 2020.

VERIFY is a research project funded by the European Commission under the H2020 program. Grant Agreement number 776810.

the middle between the TNO CO/ffCO$_2$ emission ratios for all traffic (green) and highway traffic only (black). All inventory-based NO$_x$/ffCO$_2$ emission ratios are (slightly) higher than the observed atmospheric ratios. While the TNO-based NO$_x$/ffCO$_2$ emission ratios fit well, StaLA and LUBW clearly overestimate the ratio. Figure 6.11 compares the measured ratios to the TNO-based emission ratios in the double-ratio plot. The TNO-based traffic emissions ratios are shown for the average fuel and road mix (traffic mix) as well as separated by fuel type. In addition, traffic emission ratios for highways are shown. According to the TNO inventory, the NO$_x$/ffCO$_2$ emission ratios do not change for the different road types. The CO/ffCO$_2$ emission ratios of diesel vehicles change only slightly for different road types. However, gasoline vehicles' CO/ffCO$_2$ emission ratio changes enormously with road type and associated engine operating conditions and driving conditions. The observed atmospheric ratios scatter between the inventory-based emission ratios for highway- and mixed traffic conditions. The weighted mean atmospheric traffic ratios agree within their uncertainties to the mixing line (dashed) between gasoline and diesel vehicles for motorway driving conditions but differ from the TNO-predicted mean highway emission ratio. The small number of usable atmospheric measurements prohibits a more in-depth analysis of the differences. Possible causes for the difference are a) different fleet composition between

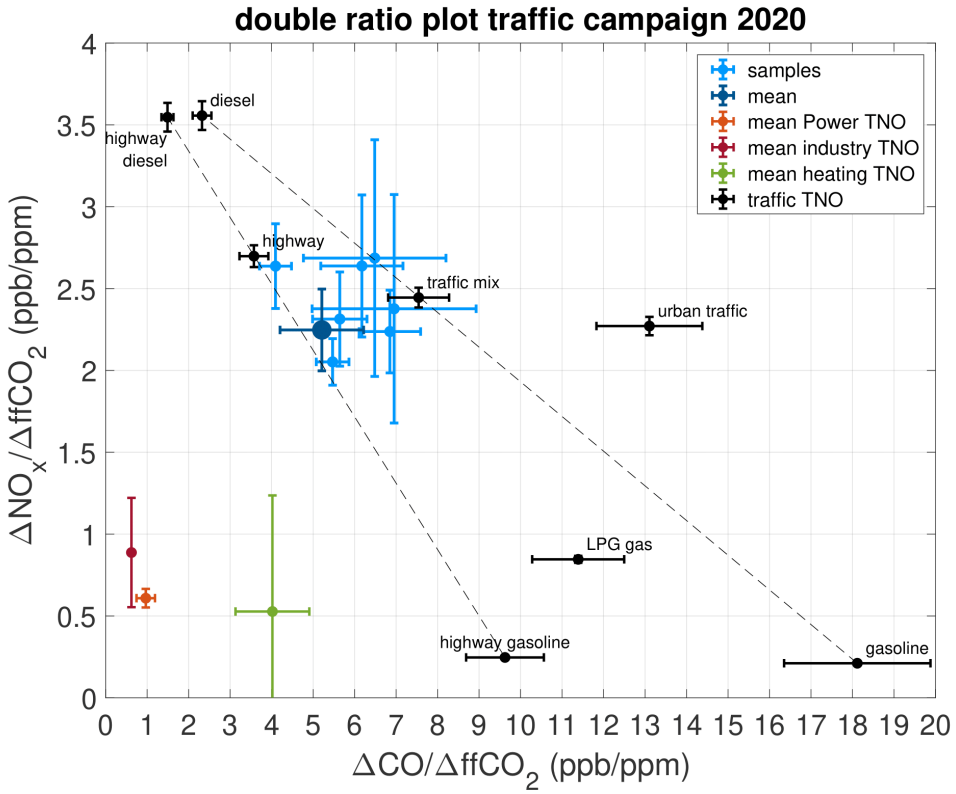

Figure 6.11 Sector-specific double ratios for the traffic campaign. For reference, emission ratios from TNO (mean of four sectors in a 50 km x 50 km square around Heidelberg) are shown. The dashed lines represent possible fleet compositions (from all-diesel to all-gasoline compositions).

VERIFY is a research project funded by the European Commission under the H2020 program. Grant Agreement number 776810.

inventory and reality[11] and b) differences in fuel-specific and road-type specific emission ratios. Also, the below-average truck traffic volume for this highway section can explain why the observed ratios are more in line with an increased gasoline ratio [BASt, 2017].

[11] The TNO inventory uses one year of OpenStreetMap and OpenTransportMap to assess fleet composition. This data may be outdated [personal communication Stijn Dellaert, 07.05.2021]

VERIFY is a research project funded by the European Commission under the H2020 program. Grant Agreement number 776810.

6.3. Traffic sector (total column)

6.3.1. Campaign location and setup

The total-column campaign aimed to quantify the emissions released from a section of the A5 highway in the area of the city of Bruchsal, as shown in Figure 6.12.
One spectrometer was located in the village Büchenau (instrument 1 in Figure 6.12): 49.104 °N, 8.533 °E and an altitude of ≈115 m asl to the West of the highway, while the other spectrometer was located in the village Untergrombach (Instrument 2 in Figure 6.12): 49.092 °N, 5.550 °E and an altitude of ≈ 112 m asl, to the East of the highway. In one site, unobstructed observational conditions (line-of-sight towards sun free of trees, buildings and any other kind of obstructions), which is required for the measurements, were realised only in the afternoon due to obstructions that hindered measurements in the morning (instrument 1, located at Büchenau).

Figure 6.12 Map with the location of the instruments over a section of the A5 motorway.

Table 6.6 Instrument-to-instrument calibration factors obtained from the side-by-side measurements for both instruments with respect to the COCCON's reference instrument.

Date	Spectrometer serial number	Calibration factor XCO_2	Calibration factor XCO
02-06-2020	81	0.99992016	1.01169965
07-09-2020	81	0.99996096	1.00703221
02-06-2020	97	0.99825419	1.01227831
07-09-2020	97	0.99822649	1.00622572

VERIFY is a research project funded by the European Commission under the H2020 program. Grant Agreement number 776810.

A crucial point when measuring small differential signals is attempted is the careful calibration of the spectrometers involved. For this purpose and for ensuring the stability of the instruments during the campaign period, the EM27/SUN spectrometers were inter-calibrated before and after the campaigns side-by-side, including measurements in comparison to the primary EM27/SUN operated continuously next to the TCCON spectrometer in Karlsruhe. The calibration procedures are described by Frey et al. [Frey et al., 2019]. From these measurements, the calibration factors for each instrument were derived and are listed in Table 6.6. These factors are applied in the calculation of the differential column signals. As evident from the table, the spectrometers were highly stable in their instrumental characteristics.

6.3.2. Results

For recording solar absorption measurements, sunny weather conditions are a prerequisite: from June to August, a total of 10 days of measurements were collected successfully with the two spectrometers. Figure 6.13 provides an overview of all measurements collected. The one-sigma precision of the XCO_2 measurement is in the order of 0.06 ppm, while the 1σ precision of the XCO measurement is in the order of 0.3 ppb (integration time is one minute).

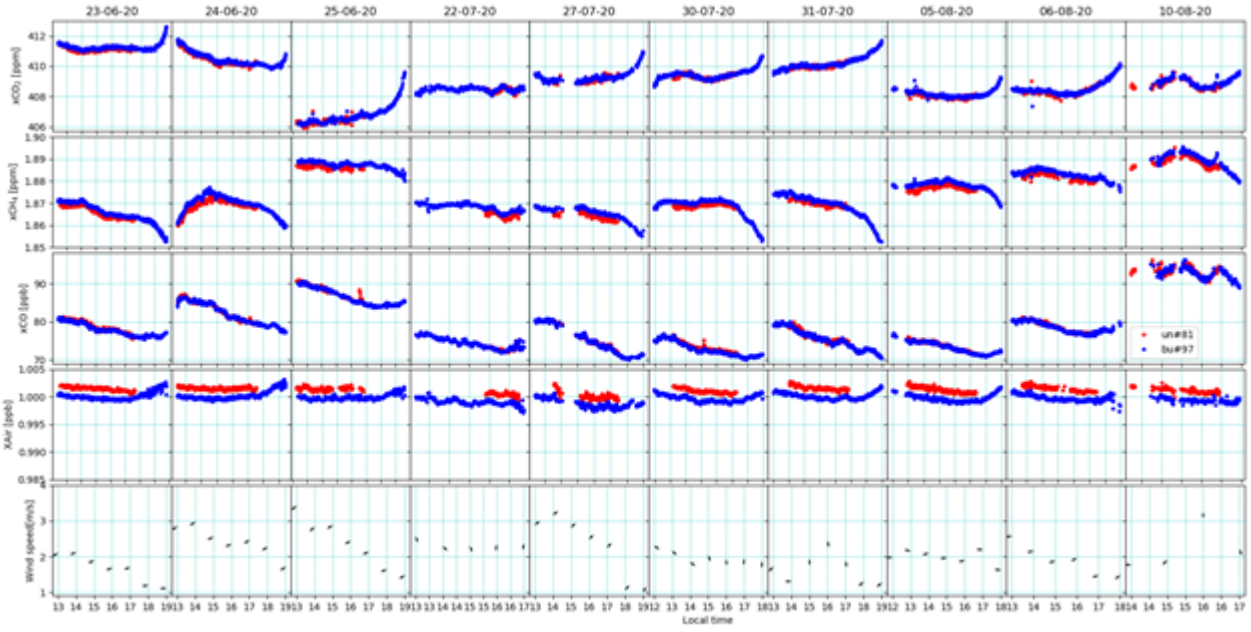

Figure 6.13 General overview of the entire campaign results. The column-averaged dry-air mixing ratios of CO_2 and CO denoted as XCO_2 and XCO are shown in the first and third rows. The last row shows wind speed and direction

In Figures 6.14 and 6.15, we present two days as an example. By re-sampling, the time series recorded with the pair of spectrometers to a common time grid, the differences between the column-averaged CO and CO_2 measurements can be calculated (ΔXCO and ΔXCO_2) as function of time. The final step is correlating the resulting ΔXCO data with the associated ΔXCO_2 data.

Unfortunately, no clear correlation between ΔXCO and ΔXCO$_2$ can be established from this analysis (see Figure 6.16). We, therefore, conclude that the signals generated by a single highway are too weak to be detectable with the remote sensing approach. We can estimate a typical XCO$_2$ signal from a highway (assuming a total bi-directional traffic density along the highway of 10 cars/s and 5 trucks/s and a 2.5 m/s wind component orthogonal to the road) to be in the order of 0.02 ppm (so we would expect XCO signal around 0.14 ppb). A correlated signal of this amplitude would be hardly visible in Figure 6.16.

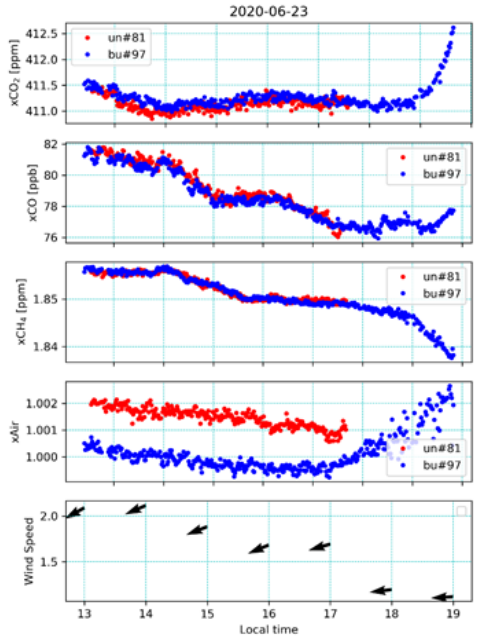

Figure 6.14 example day: 23/06/2020

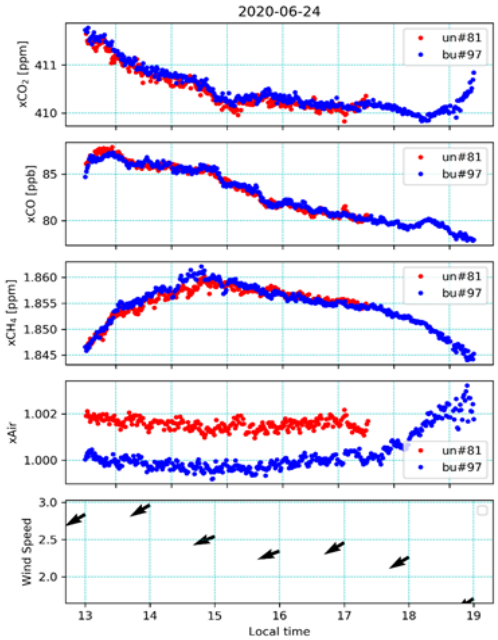

Figure 6.15 example day: 24/06/2020

VERIFY is a research project funded by the European Commission under the H2020 program. Grant Agreement number 776810.

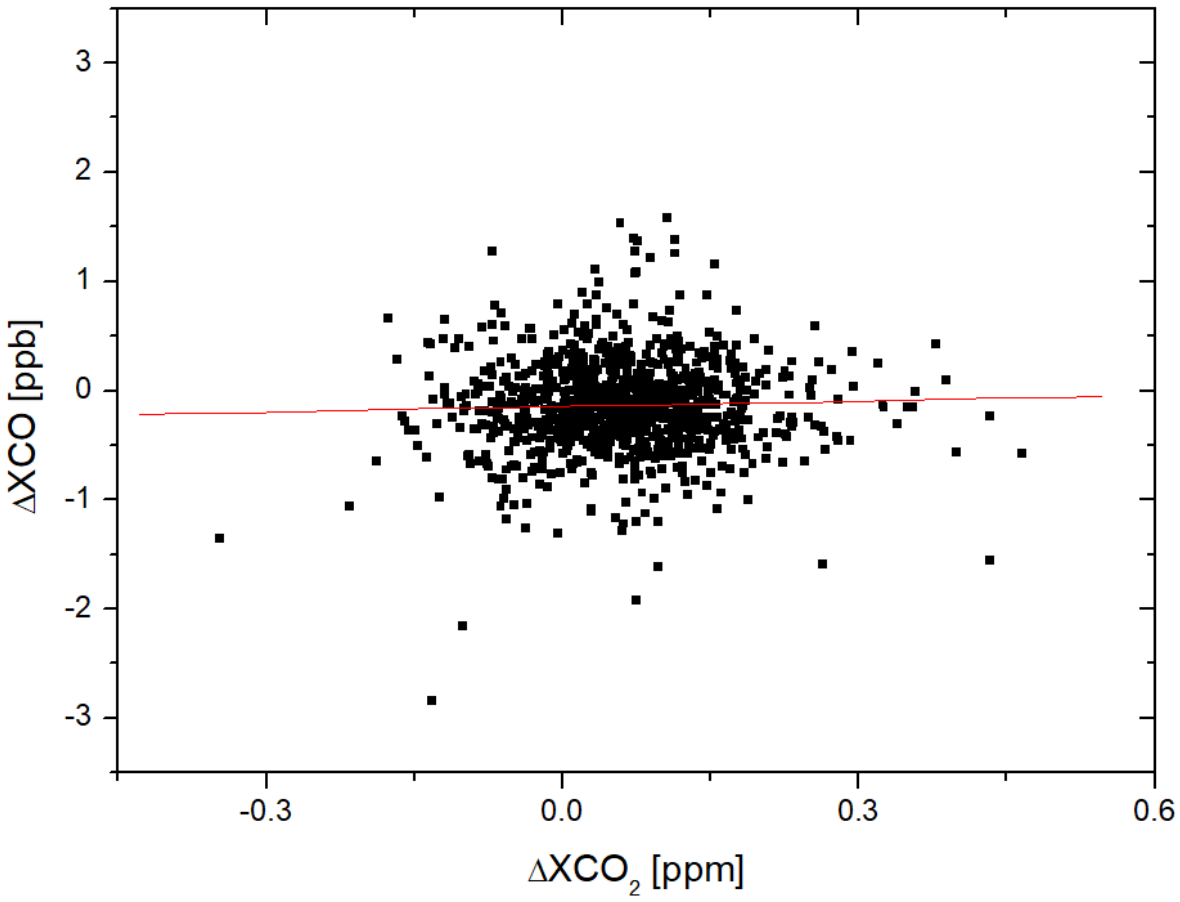

Figure 6.16 This plot of ΔXCO as function of ΔXCO2 does not reveal any significant correlation (regression line has a slope of 0.17 ± 0.15 with R = 0.036)

7. Conclusions

One in-situ campaign measured effective atmospheric Δproxy/ΔffCO$_2$ emission ratios for the residential heating sector during late winter/early spring 2020 using the single-station approach. The weighted means and weighted standard deviations of the atmospheric enhancement ratios are:

$$\Delta CO/\Delta ffCO_{2\ (heating)} = 6.5 \pm 2.6 \text{ ppb/ppm}$$
$$\Delta NO_x/\Delta ffCO_{2\ (heating)} = 0.8 \pm 0.2 \text{ ppb/ppm}$$

Especially for the mean $\Delta CO/\Delta ffCO_{2\ (heating)}$ ratio, we observe a large variability of 40% (1σ) that is, however, expected as the different heating fuel-types (oil, gas and wood) produce very different CO/ffCO$_2$ emission ratios. The variability in the atmospheric $\Delta NO_x/\Delta ffCO_2$ ratio is at the same time, less than 20% (1σ). Both Δproxy/ΔffCO$_2$ ratios are 2 to 4 times larger than the inventory predicted local emission ratios. This misfit decreases to about 50% underestimation of

VERIFY is a research project funded by the European Commission under the H2020 program. Grant Agreement number 776810.

the TNO inventory when compared to the average residential heating emissions in the 50 km x 50 km square around Heidelberg. The variability of the atmospheric ratios is significantly higher for $\Delta CO/\Delta ffCO_2$ and significantly lower for $\Delta NO_x/\Delta ffCO_2$ than predicted by the TNO inventory. The variability of the emission ratios in reality and in the inventories should be further investigated, especially since this variability is transferred one-to-one into the uncertainty of the proxy-based $ffCO_2$ estimates.

We measured effective atmospheric $\Delta proxy/\Delta ffCO_2$ ratios for the traffic sector during the in-situ campaign in autumn 2020 and winter 2021 using the two-station approach. The weighted mean $\Delta proxy/\Delta ffCO_2$ ratios with their weighted standard deviation are:

$$\Delta CO/\Delta ffCO_{2\,(traffic)} = 5.21 \pm 1.01 \text{ ppb/ppm}$$
$$\Delta NO_x/\Delta ffCO_{2\,(traffic)} = 2.24 \pm 0.25 \text{ ppb/ppm}$$

The atmospheric traffic ratio is within its uncertainties on the mixing line between the emission ratios of diesel and gasoline vehicles on highways but is shifted more towards gasoline vehicles. According to the traffic agency BASt [2017], the investigated highway section has a below-average truck traffic volume, which could explain the observed shift. A more in-depth validation of the traffic emission ratio requires comparing the fuel-type specific activity data between inventory and experiment, which is beyond the scope of this study.

For remote sensing, determining an $\Delta XCO/\Delta XCO_2$ ratio from a single highway using near-infrared solar spectra turns out to be not feasible even with the most efficient sensors available today. The signals are below the detection threshold. Even if the measurement precision could be further improved, it remains questionable whether the highway source would dominate the detected correlation. More likely, the approach would still be prone to advected contaminations. Therefore, future attempts to use infrared spectroscopy should consider open-path instead of solar observations.

VERIFY is a research project funded by the European Commission under the H2020 program. Grant Agreement number 776810.

8. References

Ammoura, L., Xueref-Remy, I., Gros, V., Baudic, Bonsang, B., A., Petit, J.-E., Perrussel, O. Bonnaire, N., Sciare, J., Chevallier, F. (2014). Atmospheric measurements of ratios between CO_2 and co-emitted species from traffic: a tunnel study in the Paris megacity. Atmospheric Chemistry and Physics, 14(23), 12871–12882. doi: 10.5194/acp-14-12871-2014

BASt (2017). https://www.bast.de/BASt_2017/DE/Verkehrstechnik/Fachthemen/v2-verkehrszaehlung/Aktuell/zaehl_aktuell_node.html, last called: 20.04.2021

Bava, L., Zucali, M., Sandrucci, A., & Tamburini, A. (2017). Environmental impact of the typical heavy pig production in Italy. Journal of Cleaner Production, 140, 685 - 691. Retrieved fromhttp://www.sciencedirect.com/science/article/pii/S0959652615016686 (Towards eco-efficient agriculture and food systems: selected papers addressing the global challenges for food systems, including those presented at the Conference "LCA for Feeding the planet and energy for life" (6-8 October 2015, Stresa & Milan Expo, Italy)) doi: https://doi.org/10.1016/j.jclepro.2015.11.029

Bishop, G. A., & Stedman, D. H. (2008). A decade of on-road emissions measurements. Environmental Science and Technology, 42(5), 1651–1656. doi: 10.1021/es702413b

Chen, J., Viatte, C. , Hedelius, J. K. , Jones, T. , Franklin, J. E. , Parker, H. , Gottlieb, E. W. , Wennberg, P.O. , Dubey, M.K. , Wofsy, S.C. (2016) Differential column measurements using compact solar-tracking spectrometers, Atmos. Chem. Phys., 16, 8479–8498, 2016

Doerr, H., & Münnich, K. (1986). Annual variations of the ^{14}C content of soil CO_2. Radiocarbon, 28(2A), 338–345.

EEA (2019). EMEP/EEA air pollutant emission inventory guidebook 2019. EEA Report No 13/2019. Available at: https://www.eea.europa.eu/publications/emep-eea-guidebook-2019 (08-09-2020)

Frey, M., Sha, M. K., Hase, F., Kiel, M., Blumenstock, T., Harig, R., Surawicz, G., Deutscher, N. M., Shiomi, K., Franklin, J. E., Bösch, H., Chen, J., Grutter, M., Ohyama, H., Sun, Y., Butz, A., Tsidu, G. M., Ene, D., Wunch, D., Cao, Z., Garcia, O., Ramonet, M., Vogel, F., Orphal, J. (2019). Building the COllaborative Carbon Column Observing Network (COCCON): long-term stability and ensemble performance of the EM27/SUM Fourier transform spectrometer.

Friedrich, R & Hammer, S (2017). How much bio is in fuel? 10th International Carbon Dioxide Conference, Interlaken, Switzerland

VERIFY is a research project funded by the European Commission under the H2020 program. Grant Agreement number 776810.

Gadd, H., & Werner, S. (2013). Heat load patterns in district heating substations. Applied Energy, 108, 176 - 183. Retrieved from http://www.sciencedirect.com/science/article/pii/S0306261913001803 doi: https://doi.org/10.1016/j.apenergy.2013.02.062

Gisi, M., Hase, F., Dohe, S., Blumenstock, T., Simon, A., and Keens, A.: XCO2-measurements with a tabletop FTS using solar absorption spectroscopy, Atmos. Meas. Tech., 5, 2969–2980, doi:10.5194/amt-5-2969-2012, 2012.

Glarborg, P., Miller, J. A., Ruscic, B., & Klippenstein, S. J. (2018). Modeling nitrogen chemistry in combustion. Progress in Energy and Combustion Science, 67, 31–68. Retrieved from https://doi.org/10.1016/j.pecs.2018.01.002 doi: 10.1016/j.pecs.2018.01.002

Hase, F., Frey, M., Kiel, M., Blumenstock, T., Harig, R., Keens, A., & Orphal, J. (2016). Addition of a channel for XCO observations to a portable FTIR spectrometer for greenhouse gas measurements. Atmospheric Measurement Techniques, 9(5), 2303–2313.

Heitkoetter, W., Medjroubi, W., Vogt, T., & Agert, C. (2020). Regionalised heat demand and power-to-heat capacities in Germany – An open dataset for assessing renewable energy integration. Applied Energy, 259(June 2019), 114161. Retrieved from https://doi.org/10.1016/j.apenergy.2019.114161 doi: 10.1016/j.apenergy.2019.114161

Horbanski, M., Pöhler, D., Lampel, J., & Platt, U. (2019). The ICAD (iterative cavity-enhanced DOAS) method. Atmospheric Measurement Techniques, 12(6), 3365–3381. doi: 10 .5194/amt-12-3365-2019

Karstens, U., Schwingshackl, C., Schmithüsen, D., & Levin, I. (2015). A process-based 222 radon flux map for Europe and its comparison to long-term observations. Atmospheric Chemistry and Physics, 15(22), 12845-12865.

Kenagy, H. S., Sparks, T. L., Ebben, C. J., Wooldrige, P. J., Lopez-Hilfiker, F. D., Lee, B. H., . . . Cohen, R. C. (2018). NO_x Lifetime and NO_y Partitioning During WINTER. Journal of Geophysical Research: Atmospheres, 123(17), 9813–9827. doi: 10.1029/2018JD028736

Ko, J., Son, J., Myung, C.-L., & Park, S. (2018). Comparative study on low ambient temperature regulated/unregulated emissions characteristics of idling light-duty diesel vehicles at cold start and hot restart. Fuel, 233, 620 - 631. Retrieved from http://www.sciencedirect.com/science/article/pii/S0016236118309803 doi: https://doi.org/10.1016/j.fuel.2018.05.144

Konovalov, I. B., Berezin, E. V., Ciais, P., Broquet, G., Zhuravlev, R. V., & Janssens-Maenhout, G. (2016). Estimation of fossil-fuel CO_2 emissions using satellite measurements of "proxy" species. Atmospheric Chemistry and Physics, 16(21), 13509–13540. doi: 10.5194/acp-16-13509-2016

Levin, I., Born, M., Cuntz, M., Langendörfer, U., Mantsch, S., Naegler, T., Schmidt, M., Varlagin, A., Verclas, S., Wagenbach, D. (2002). Observations of atmospheric variability and soil exhalation rate of Radon-222 at a russian forest site. technical approach and deployment for boundary layer studies. Tellus B, 54(5), 462-475. Retrieved from https://onlinelibrary.wiley.com/doi/abs/10.1034/j.1600-0889.2002.01346.x doi: https://doi.org/10.1034/j.1600-0889.2002.01346.x

Levin, I., Hammer, S., Kromer, B., & Meinhardt, F. (2008). Radiocarbon observations in atmospheric CO_2: Determining fossil fuel CO_2 over Europe using Jungfraujoch observations as background. Science of the Total Environment, 391(2-3), 211–216. doi: 10.1016/j.scitotenv.2007.10.019

Levin, I., & Karstens, U. (2007). Inferring high-resolution fossil fuel CO2 records at continental sites from combined $^{14}CO_2$ and CO observations. Tellus, Series B: Chemical and Physical Meteorology, 59(2), 245–250. doi: 10.1111/j.1600-0889.2006.00244.x

Mook, W. (1986). ^{13}C in atmospheric CO_2. Netherlands Journal of Sea Research, 20(2-3), 211–223.

Reuter, M., Buchwitz, M., Schneising, O., Krautwurst, S., O'Dell, C. W., Richter, A., Bovensmann, H., Burrows, J. P. (2019). Towards monitoring localised CO_2 emissions from space: co-located regional CO_2 and NO_2 enhancements observed by the OCO-2 and S5P satellites. Atmos. Chem. Phys., 19(14), 9371–9383. Retrieved from https://acp.copernicus.org/articles/19/9371/2019/ doi: https://doi.org/10.5194/acp-19-9371-2019

Rukhin, A. L. (2009). Weighted means statistics in interlaboratory studies. Metrologia, 46(3), 323–331. doi: 10.1088/0026-1394/46/3/021

Seinfeld, J. H., & Pandis, S. N. (2016). Atmospheric chemistry and physics: from air pollution to climate change. John Wiley & Sons.

Shah, V., J. Jacob, D., Li, K., Silvern, R., Zhai, S., Liu, M., Lin, J., Zhang, Q. (2020). Effect of changing NO_x lifetime on the seasonality and long-term trends of satellite- observed tropospheric NO_2 columns over China. Atmospheric Chemistry and Physics, 20(3), 1483–1495. doi: 10.5194/acp-20-1483-2020

Smooke, M., Ern, A., Tanoff, M. A., Valdati, B. A., Mohammed, R. K., Marran, D., & Long, M. (1996). Computational and experimental study of NO in an axisymmetric laminar diffusion flame, 2161–2170. doi: 10.1016/S0082-0784(96)80042-7

VERIFY is a research project funded by the European Commission under the H2020 program. Grant Agreement number 776810.

Stuvier, M., & Polach, H. A. (1977). Reporting of ^{14}C data. Radiocarbon, 19(3), 355-363.

Super, I., Dellaert, S. N. C., Visschedijk, A. J. H., and Denier van der Gon, H. A. C. (2020). Uncertainty analysis of a European high-resolution emission inventory of CO_2 and CO to support inverse modelling and network design, Atmos. Chem. Phys., 20, 1795–1816, https://doi.org/10.5194/acp-20-1795-2020

Turnbull, J. C., Sweeney, C., Karion, A., Newberger, T., Lehman, S. J., Tans, P. P., Davis, K. J., Lauvaux, T., Miles, N. L., Richardson, S. J., Cambaliza, M. O., Shepson, P. B., Gurney, K., Patarasuk, R., Razlivanov, I. (2015). Toward quantification and source sector identification of fossil fuel CO_2 emissions from an urban area: Results from the influx experiment. Journal of Geophysical Research: Atmospheres, 120(1), 292-312. Retrieved from https://agupubs.onlinelibrary.wiley.com/doi/abs/10.1002/2014JD022555 doi: https://doi.org/10.1002/2014JD022555

Turner, D.B. , "Workbook of Atmospheric Dispersion Estimates," EPA, Research Triangle Park, NC, 1970.

Vollmer, M. K., Juergens, N., Steinbacher, M., Reimann, S., Weilenmann, M., & Buchmann, B. (2007). Road vehicle emissions of molecular hydrogen (H_2) from a tunnel study. Atmospheric Environment, 41(37), 8355–8369. doi: 10.1016/j.atmosenv.2007.06.037

Vollmer, M.K., Popa, M.E., Jordan, A., Brand, W.A., Pathirana, S.L., Rothe, M., & Röckmann, T. (2014). Vehicle emissions of greenhouse gases and related tracers from a tunnel study: CO:CO_2, N_2O:CO_2, CH_4:CO_2, O_2:CO_2 ratios, and the stable isotopes ^{13}C and ^{18}O in CO_2 and CO. Atmos. Chem. Phys., 14(1), 2105–2123. Retrieved from https://acp.copernicus.org/articles/14/2105/2014/acp-14-2105-2014.html doi: https://doi.org/10.5194/acp-14-2105-2014